UNIVERSIDADE DE BRASÍLIA
FACULDADE DE CIÊNCIAS DA SAÚDE

FELIPE DE QUEIROZ PIRES

DEVELOPMENT OF LIPID NANOPARTICLES LOADING THYMOL AND *Lippia origanoides* ESSENTIAL OIL IN INCLUSION COMPLEXES WITH CYCLODEXTRIN

BRASÍLIA
2018

UNIVERSIDADE DE BRASÍLIA
FACULDADE DE CIÊNCIAS DA SAÚDE
PROGRAMA DE PÓS-GRADUAÇÃO EM CIÊNCIAS FARMACÊUTICAS

FELIPE DE QUEIROZ PIRES

DEVELOPMENT OF LIPID NANOPARTICLES LOADING THYMOL AND *Lippia origanoides* ESSENTIAL OIL IN INCLUSION COMPLEXES WITH CYCLODEXTRIN

Dissertação apresentada como requisito parcial para a obtenção do Título de Mestre em Ciências Farmacêuticas pelo Programa de Pós-Graduação em Ciências da Farmacêuticas da Universidade de Brasília.

Orientador: Marcílio Sérgio Soares da Cunha Filho

Co-orientadora: Tais Gratieri

BRASÍLIA
2018

d D489d

de Queiroz Pires, Felipe
DEVELOPMENT OF LIPID NANOPARTICLES LOADING THYMOL AND Lippia origanoides ESSENTIAL OIL IN INCLUSION COMPLEXES WITH CYCLODEXTRIN / Felipe de Queiroz Pires; orientador Marcílio Sérgio Soares da Cunha Filho ; co-orientador Tais Gratieri. -- Brasília, 2018.
85 p.

Dissertação (Mestrado - Mestrado em Ciências Farmacêuticas) -- Universidade de Brasília, 2018.

1. Pré-formulação. 2. Nanopartículas lipídicas. 3. Timol. 4. Ciclodextrina. 5. Óleo Essencial. I. Soares da Cunha Filho , Marcílio Sérgio , orient. II. Gratieri, Tais, co orient. III. Título.

Felipe de Queiroz Pires

Development of lipid nanoparticles loading thymol and Lippia origanoides essential oil in inclusion complexes with cyclodextrin

Aprovado em 21 de fevereiro de 2018

Banca Examinadora

Prof. Dr. Marcílio Sérgio Soares da Cunha Filho – Universidade de Brasília

Dra. Zênia Maria Maciel Lavra – Ministério da Saúde

Prof. Dr. Guilherme Martins Gelfuso – Universidade de Brasília

AGRADECIMENTOS

Agradeço aos meus pais e minha irmã por todo apoio, confiança e paciência. Minhas primas e amigas Amanda, Gabriela e Tamara, pelo apoio psicológico e pela força extra.

Agradeço ao meu orientador, professor Marcílio Cunha-Filho pela orientação e o esforço em moldar este trabalho até a melhor forma possível. À professora Taís Gratieri pela colaboração intelectual. Ao professor Guilherme Gelfuso pela colaboração tanto intelectual quanto pessoal, incentivando a manutenção do bom trabalho e todos os outros professores e profissionais que colaboraram com o trabalho.

E por fim, agradeço aos meus colegas do LTMAC, em especial à Tamara Ângelo, Lorena Malaquias, Ludmila Alvim, Maíra Nunes, Breno Noronha, Paula Martins, Maíra Teixeira e Ricardo Nunes que não só me ajudaram em diversos experimentos, mas contribuíram sempre com ideias e palavras de incentivo.

“Fairy tales are more than true: not because they tell us that dragons exist, but because they tell us that dragons can be beaten.”

(Neil Gaiman)

RESUMO

O objetivo desse estudo foi a confecção de carreadores lipídicos nanoestruturados utilizando como componente ativo a forma complexada do timol e do óleo essencial de *Lippia origanoides* em ciclodextrinas, para utilização em sistemas de administração tópica com potencial para tratamento de distúrbios de pele. A primeira parte do trabalho consistiu na obtenção de um método analítico cromatográfico seletivo para determinação de timol em estudos *in vitro* de permeação na pele. O método desenvolvido apresentou elevada capacidade de recuperação do timol das camadas da pele e provou ser adequado segundo todos os parâmetros de validação avaliados. A segunda parte consistiu em um estudo de pré-formulação utilizando desenho experimental de mistura visando avaliar a compatibilidade dos componentes da formulação do nanocarreador lipídico. A partir desses estudos foram definidos os excipientes as serem usados na fase seguinte, excluindo o tensoativo taurodeoxicolato de sódio que apresentou ação sinérgica com outros componentes reduzindo a estabilidade do timol. A terceira parte do trabalho consistiu na obtenção de complexos de inclusão de timol e óleo essencial a partir de uma seleção diferentes ciclodextrinas e métodos de obtenção de complexos de inclusão em estado sólido. Os resultados mostraram que a 2-hidroxipropil-β-ciclodextrina foi capaz de formar um complexo mais estável com o timol e que o processo de liofilização conseguiu produzir um material com maiores evidências de encapsulação, tanto para o timol, quanto para o óleo essencial, com maior estabilidade térmica e melhor solubilidade. Na parte final do trabalho, carreadores lipídicos nanoestruturados foram produzidos a partir da forma livre e complexada de timol e óleo essencial obtidos por liofilização. Comparando com a solução padrão dos ativos, todos os nanocarreadores foram capazes de controlar a liberação e a permeação do timol nas camadas da pele, sendo os nanocarreadores confeccionados com o complexo de inclusão capazes de reter completamente o componente ativo nas camadas iniciais da pele. Assim, os sistemas de liberação desenvolvidos apresentaram estabilidade e capacidade de controlar a liberação do timol e óleo essencial evidenciando grande potencial de aplicação farmacêutica.

Palavras-chave: Timol, *Lippia origanoides*, Ciclodextrina, Complexos de inclusão Carreadores lipídicos nanoestruturados.

ABSTRACT

The objective of this study was the preparation of nanostructured lipid carriers using as an active component the complexed form of thymol and the essential oil of *Lippia origanoides* in cyclodextrins for use in topical delivery systems with potential for the treatment of skin disorders. The first part of the work consisted of obtaining a selective chromatographic analytical method for the determination of thymol *in vitro* studies of permeation in the skin. The developed method presented a high recovery capacity of thymol from the skin layers and proved to be adequate according to all the validation parameters tested. The second part consisted of a preformulation study using experimental mixing design to evaluate the compatibility of components of the lipid nanocarrier formulation. From these studies were defined the excipients to be used in the next phase, excluding the sodium taurodeoxycholate surfactant that presented synergistic action with other components reducing the thymol stability. The third part of the work consisted of obtaining inclusion complexes of thymol and essential oil from a selection of different cyclodextrins and methods of obtaining solid inclusion complexes. The results showed that 2-hydroxypropyl-β-cyclodextrin was able to form a more stable complex with thymol and that the lyophilization process was able to produce a material with higher evidence of encapsulation with both thymol and essential oil, with higher thermal stability and better solubility. In the final part of the work, nanostructured lipid carriers were produced from the free and complexed form of thymol and essential oil obtained by lyophilization. Compared with the solution containing the active compounds, all nanocarriers were able to control the release and permeation of thymol in the skin layers, and the nanocarriers made with the inclusion complex were able to completely retain the active component in the initial layers of the skin. Thus, the delivery systems developed showed stability and ability to control the release of thymol and essential oil evidencing great potential for pharmaceutical application.

Keywords: Thymol, *Lippia origanoides*, Cyclodextrin, Inclusion Complexes, Nanostructured Lipid Carriers.

LIST OF FIGURES

LIST OF TABLES

LIST OF ABREVIATIONS

CAPES	Coordenação de Aperfeiçoamento de Pessoal de Nível Superior
CD	Cyclodextrin
CE	Complexation efficiency
CNPQ	Conselho Nacional de Desenvolvimento Científico e Tecnológico
DL	Drug Loading
DP	Dissolution profile
DrTG	First derivative of TGA
DSC	Differential scannin calorimetry
DTA	Differential thermal analysis
EE	Encapsulation Efficiency
EO	Essential Oil
FAP-DF	Fundação de Apoio a Pesquisa do Distrito Federal
FD	Freeze Drying
FDA	Food and drug administration
FF	Filtered Fraction
FTIR	Fourier Transformed infrared spectroscopy
HPLC	High profile liquid chromatography
HPβCD	Hydroxypropyl-β-cyclodextrin
LC	Soybean lecytin
LOD	Limit of detection
LOQ	Limit of quantification
NLC	Nanostructured lipid carrier
P80	Polysorbate 80
PDI	Polydispersity index
PM	Physical mixture
RE	Rotary Evaporation
RS	Remain skin
RT	Retention time
SA	Stearic acid
SC	Stratum cornius
$SCCO_2$	Supercritical CO_2

SD	Spray Drying
SEM	Scanning electron microscopy
TAU	Sodium Taurodeoxycolat
TC	Theoretical concentration
TD	Total drug
TGA	Termogravimetry
TL	Total lipid
TML	Thymol
UV	Ultraviolet

SUMMARY

CHAPTER 1 - JUSTIFICATION AND LITERATURE REVIEW

1.1 INTRODUCTION

Thymol (TML) is a monoterpene presents as a majority compound in the essential oils of several plants. This molecule, in isolated form or in natural extracts, has a large spectra of pharmacological activities, such as antioxidant, antimicrobial, cicatrizing and protective action against damages of UV radiation (KAVOOSI; DADFAR; PURFARD, 2013; MARCHESE et al., 2016; PEREZ-VASQUEZ et al., 2011; RIELLA et al., 2012). Despite the vast therapeutic potential of TML, its pharmaceutical use, particularly in skin topical treatments, is practically unexplored.

The first step to enable the TML administration to the skin is to find a selective analytical method capable of quantifying the drug extracted from the skin, since this complex organ has many contaminants that may interfere with the analysis. Although literature has already reported some chromatographic methods for TML assaying (CHEN; CHEN, 2012; HAJIMEHDIPOOR et al., 2010; LI; YUAN; SU, 2006; SOLINAS; GESSA; DELITALA, 1981), none of them evaluated drug selectivity in the presence of possible skin interferents.

The unfavorable physicochemical characteristics of TML, mainly its volatility, light sensitivity and low water solubility is a decisive issue which needs to be overcome for its therapeutic exploitation. In this sense, TML complexation with cyclodextrins (CDs) has proved to be a very promising approach (ABARCA et al., 2015; BETHANIS et al., 2013; LOCCI et al., 2004; MARRETO et al., 2008; MULINACCI et al., 1996; RASSU et al., 2014; TAO et al., 2014).

Moreover, for TML topical use, it is also necessary to insert this drug in a controlled release system capable of interacting with the skin and promoting the drug control release directed to the superficial layers of the skin in order to avoid an undesired systemic absorption (CHANTASART et al., 2009; GELFUSO; CUNHA-FILHO; GRATIERI, 2016).

In this context, the nanostructured lipid carriers (NLCs) formed by solid and liquid lipids, which are the most modern generation of lipid nanoparticles, with more stability and higher drug loading capacity, emerges as a promising alternative (GELFUSO; CUNHA-FILHO; GRATIERI, 2016). In fact, NLCs have been used successfully in enhance the skin permeation of several drugs (CHAUDHARI, 2012), however, there is no studies involving the use of NLC with TML or natural extracts containing this compound. Nevertheless, the high reactivity of the lipid components (SHAHIDI; ZHONG, 2010; SILVA et al., 2016), could

compromise NLC over-all stability. In such context, compatibility studies between TML and lipid excipients are strongly demanded.

1.2 OBJECTIVES

Development of a nanostructured lipid carrier functionalized with the complex of TML and *Lippia origanoides* essential oil with cyclodextrin.

1.2.1 Specific objectives

- Develop and validate a chromatographic analytical method suitable for the determination of TML in drug delivery systems and to be use in skin permeation studies of TML topical formulations;
- Evaluate the drug-excipient compatibility between TML and NLC excipients using thermal and spectroscopic analyses following a mixture design;
- Select the best cyclodextrin type for complexation of TML and EO based on phase-solubility studies;
- Select the most suitable methodology for obtaining solid inclusion complexes considering several physicochemical properties, such as scanning electron microscopy, infrared spectroscopy, thermal analysis and dissolution rate;
- Prepare NLC of TML and EO in free and in inclusion complexed forms and analyze these systems by physicochemical assays, as well as liberation and permeation studies.

1.3 LITERATURE REVIEW

1.3.1 Skin disorders

In an adult, the skin has a total area between 18,000 cm^2 and 25,000 cm^2 and works as a barrier, avoiding the direct contact of the internal areas of the body with external agents. The skin is composed, fundamentally, of three layers, epidermis, dermis and hypodermis, been the first one the focus point for the topical drug delivery (LAUTERBACH; MÜLLER-GOYMANN, 2014; MONTENEGRO et al., 2016).

The epidermis is the most external skin layer. The cellular arrangement results in a compact and almost impermeable barrier, perfured only by the follicle polisebasea pores and the sweat glands. The stratum corneum, the outermost layer of the epidermis act to counteract

the loss of salts and water from the skin and the penetration of water soluble substances, having an important role in the protection of the body. In order to transpose the stratum corneous, the substances have to present a high liposolubility or have mechanisms that are capable to affect the cellular structure (LAUTERBACH; MÜLLER-GOYMANN, 2014).

The epidermis is a non-vascular area, so all the nutrition is provided by the more internal layers of the skin, particularly the dermis. Both the dermis and the hypodermins, because of the vascularizarion, are targets for drugs with systemic effects, but in topical drug delivery the contact with does layers have to be avoided, since, in this case, a systemic effect is considered toxic (GELFUSO; CUNHA-FILHO; GRATIERI, 2016).

The skin is constantly in contact with te external agents and that makes it vunerable, making the skin desorders one of the most common pathological conditions in humans. Affecting about 70% of the population, these disturbs can, slowly, reduce the quality of life of the individuals and, in critical cases, lead to incapacitation and death (BASRA; SHAHRUKH, 2005; BICKERS et al., 2006; FARAGE et al., 2012; HAY et al., 2014; HAY; FULLER, 2011).

Among the large variety of the skin disorders, some receive more attention, due to the severity of the symptoms and the possibility of endanger patients life, such as skin infections, melanomas and psoriasis (BASRA; SHAHRUKH, 2005; SWANSON; CANTY, 2013). However, another more common group of skin disorders with no imminent lethal risk but with clear impact on quality of life, such as acne, alopecia, irritations, degradations and many others, represent a font of shame and a psychological malaise which can evolve to more serious conditions affecting physical and mental health (GREEN, 2010).

In this sense, the research of new therapeuticals strategies to treat and prevent some of those desiases are fundamental to improve the quality of life of people who suffer from these conditions. Presenting as one of the possible strategies are the molecule Thymol.

1.3.2 Thymol

Thymol (TML, Figure 1.1), 2-isopropyl-5-methylphenol, belongs to the cyclic phenolic monoterpene class and presents in its structure two isoprene units to form of a ring with a hydroxyl group bonded in this base structure forming a phenol (CHAPPELL, 1995; KUMAR; RAWAT, 2013; TAN et al., 2016). This molecule is a biological derivative of cymene and carvacrol and is founded in essential oil of several plants as the main component (ARCHANA; NAGESHWAR; SATISH, 2011).

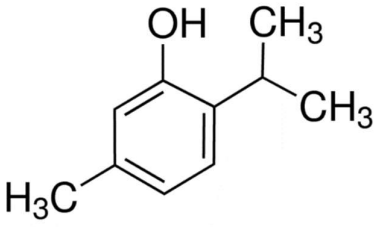

Figure 1.1 TML chemical structure (ANGELO et al., 2016)

The antiseptic, preservative and flavoring properties of TML and the essential oils containing TML explain the use of this component in food and personal care industry. In the food industry, TML are used to prevent microbiological contamination of the food inside the package during the storage process (ALTIERI et al., 2005; CASTILLO et al., 2014; KHAZAEI; ESMAIILI; EMAM-DJOMEH, 2017). TML and its natural products are also used in personal care products as an antiseptic in oral hygiene products against halitosis and as flavoring agent in several products (JENTSCH et al., 2014; PRIESTLEY et al., 2003).

Several researches proved the therapeutical benefit of TML. Traditional medicinal use of TML are described to treat several problems, such as headaches, diarrhea, cough, worms, wounds and others (KAVOOSI; DADFAR; PURFARD, 2013; LEE et al., 2005; RIELLA et al., 2012). Antibacterial, antifungal, antiparasitic, antioxidant, anti-inflammatory, local anesthetic, cardiovascular modulator, anticancer and others effects are assigned to TML (BRAGA et al., 2006; DAMASCENO et al., 2011; HAESELER et al., 2002; KANG et al., 2016; MARCHESE et al., 2016; MENDES et al., 2010; SANTOS et al., 2011; TASDEMIR et al., 2006; YANISHLIEVA et al., 1999).

In this context, the use of TML in skin preparations seems to be very promising. Moreover, some studies reported the effect of TML as skin permeation enhancer (CHANTASART et al., 2009; MOHAMMADI-SAMANI et al., 2014). This means that TML could be used not just as an active product based on drug properties already mentioned but could as well act as an auxiliary product, responsible to enhancing the delivery of actives into the skin. This perspective expands the potential of TML to cosmetic field as well.

TML physicochemical properties such as low aqueous solubility, thermal and photo sensibility represents a barrier for its pharmaceutical exploitation (SHIMODA et al., 2006). In addition, for the topical administration of this product it will be necessary to develop drug delivery systems which could be able to control its permeation through the skin.

1.3.2.1 Lippia origanoides

The genus *Lippia sp* include more than 200 species of small trees, herbs and shrubs. One of these species are the *Lippia origanoides* (Figure 1.2), a shrub native from some countries of Central America and South America, in particular, from the Amazon region. In Brazil, the main habitat of these species is in Pará state, were the plant are known by the names of "Salva de Marajó" and "Alecrim d´Angola" (OLIVEIRA et al., 2006).

Figure 1.2 *Lippia origanoides* (CALHAU, 2013)

The popular use of this plant is mainly for culinary and popular medicinal purposes. Studies pointed out that the infusion from the leaves and flowers of this plant were used in the treatment of stomachache, colic, indigestion, diarrhea, heartburn, nausea, flatus, vaginal discharge, menstrual complaints and fever. The use as antiseptic for mouth and throat is also reposted (PASCUAL et al., 2001; TELES et al., 2014).

Most of the therapeutic effects described for this plant such as antimicrobial and cicatrizing are explained by the presence of TML in large amount of this natural product. However, there are evidences that the therapeutic potential of TML could be amplified due a synergic action among the fitocomplex composition of essential oil (OLIVEIRA et al., 2006; PASCUAL et al., 2001).

1.3.3 Cyclodextrin and inclusion complexes

CD were first synthetized on France by the years of 1890s as part of the work of the pharmacist and chemist Antoine Villiers. This scientist discovered that during the process of

degradation and reduction of carbohydrates, resultant from the fermentation of potato starch, a crystal with particular properties were produced, which due to its physical and chemical similarities with cellulose was named as “cellulosine” (CRINI, 2014).

About 20 years later, the Austrian chemist and bacteriologist Franz Schardinger characterized these structures as cyclic oligosaccharides present in two different forms, distinguished by solubility and by their reaction with iodine. He decided to rename these structures as dextrins — crystalline-α-dextrin and crystalline-β-dextrin. For many years, CDs were call Schardinger dextrins, in recognition of the importance of his work in this field (CRINI, 2014; DEL VALLE, 2004).

Few years later, with the advent of crystallographic methods, the structure of the CDs was fully elucidated, and some different types of molecules were founded. It was discovered that CDs were formed by a grouping of D-glucopyranose unities arranged in a cyclic, hollow conical structure, and depending on the number of pyranose unities and the different chemical groups added to the molecule, different types of CD were formed (Table 1.1; Figure 1.3). Later these natural CDs were chemically modified by replacing their hydroxyl groups by others functional groups in order to modulate their properties. Today there are hundreds of varieties of modified CDs (MARQUES, 2010).

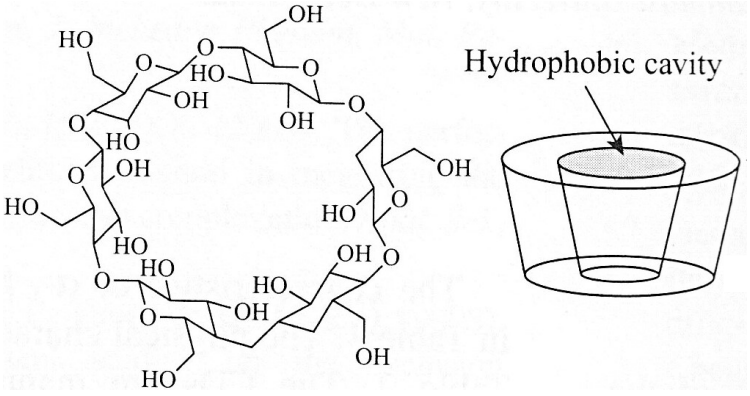

Figure 1.3 Basic chemical structure of cyclodextrin and conformation model (Adapted from HIDETOSHI; MOTOYAMA; IRIE, 2011)

In the exterior portion of the CD are located the CH groups and the polar sugar hydroxyl groups that provide a very hydrophilic characteristic to that region. In the internal portion of CD, the opposite side of the structure are located, with rings of CH groups, a glucosidic ring with oxygens donors of hydrogen bonds in the extremity and the ether oxygens, forming a

region with high hydrophobic characteristics. Based on that, two of the main properties of the CDs are explained, the water solubility of these molecules, provide by the exterior hydrophilicity; and the tendency to forming a bond with molecules with hydrophobic groups in its internal portion, forming what are called inclusion complexes (MARQUES, 2010).

Table 1.1 Types of cyclodextrins and characteristic (MARQUES, 2010).

Cyclodextrin	***Glucose unities***	***Molecular Weight (Da)***	***Cavity Dimentions (Å)***
αCD	6	972	4.5
βCD	7	1135	7.0
γCD	8	1297	8.5
δCD	9	1459	9.5

Inclusion complex are a form of chemical bond in which one molecule is encased on another molecule. The host molecule provides a protection of the included molecule, altering consequently its properties (DEL VALLE, 2004). The complexation occurs when, at the contact between the host (CD) and guest, the molecules are oriented in order to the most hydrophobic region of the guest molecule, interact with the most hydrophobic region of the CD, the internal region, and bonds are formed between the chemical groups of both structures and the result are a molecule surrounded by the CD (LOFTSSON; HREINSDÓTTIR; MÁSSON, 2005).

The complexation of guest molecules could alter substantially their properties. The exterior hydrophilic region of the CD is able to enhance the water solubility of the molecule and the structure of the CD produce a “shield effect”, protecting the molecule against external agents such as heat, light and others, enhancing considerably the molecule solubility and stability (ABARCA et al., 2015; SAMBASEVAM et al., 2013).

A relevant aspect to the CD inclusion complex formation and stability is regarding the size and tridimensional structure of guest and host (CRINI, 2014). The polarity of the guest is also important as, molecules with most hydrophobic regions on the structure are more propense to form stable inclusion complexes (MARQUES, 2010; SANTOS et al., 2015).

Moreover, studies show that many other forms of complexation are possible, such as the inclusion of more than one molecule in the same CD cavity and the non-included complexes, were the molecules interact with more external parts of the CDs. So even molecule with unfavoured characteristics to form true inclusion complexes could form a different type of

complex with CD by the interaction of functional groups (LOFTSSON; HREINSDÓTTIR; MÁSSON, 2005).

Not just the characteristic of the molecules plays an important role in the inclusion complex formation, but the preparation of these complexes can also affect the stability and strength of the bond between the molecules (SALÚSTIO et al., 2009). Specifically for the preparation of solid inclusion complexes, the methodologies which more successfully lead to inclusion complexes were freeze drying, spray drying, rotary evaporation and some more modern approaches such as supercritical fluid technology (RUDRANGI et al., 2015).

Freeze drying and spray drying are methods that involve the solubilization of the guest molecule and the CD in an aqueous solvent (mainly water) and then this solution are submitted to a drying process (SALÚSTIO et al., 2009). In the freeze drier, the solution is first frozen at very low temperature. In the equipment, a combination of a moderate heating and pressure forces the solvent sublimation until just the powder remains. The main advantages of freeze drying are the good yield of inclusion formation, the possibility of scale up the production and the use of moderate temperature making almost ideal for volatile guest molecules (SALÚSTIO et al., 2011; TAO et al., 2014).

In the spray drier, in turn, the solution is injected in the machine in liquid state. The equipment pulverizes the solution and immediately submit the resultant droplets to a high temperature treatment for a short period of time, which vaporize all the solvent. Because of the high temperature, the spray drying is recommended to be used with thermostable molecules. An advantage of this methodology is the high stability of the formed complexes. Indeed, the complexation efficiency of this method is usually high, since the instantaneously drying does not allow undo the complex previously obtained in the liquid phase (FERNANDES et al., 2009; FERNANDES; CANDIDO; OLIVEIRA, 2012).

In the rotary evaporation method, the guest molecule and the CD are solubilized in an organic solvent until the total solubilization of both. The solution is putted in a rotary evaporation equipment and a combination of high temperature and low pressure makes the solvent evaporates and leaves the sample in the powder form. Similarly as spray drying, the rotary evaporation deals with high temperature, possible not been suitable for volatile molecules, but the stability of the final product is reported to be stronger (FREITAS et al., 2012).

The supercritical fluid technology appeared as an alternative for the classic solvent methods. This technique is attractive because involves fewer steps and avoid the use of organic solvents, mostly using CO_2 in supercritical state as the main solvent. This approach is an eco-

friendly and efficient (timewise) method to produce interaction among materials in solid state (BANDI et al., 2004). Several different methods inside the supercritical fluid technology could be used to prepare an inclusion complex, depending of the characteristics of the guest and its solubility in supercritical CO_2 (DE SOUZA et al., 2017; HUANG et al., 2016; JUNIOR et al., 2017). Based in recent studies, the used of supercritical fluid is a very promising method to produce stable inclusion complexes with a broad spectra of molecules (RUDRANGI et al., 2015).

In order to evaluate the extension of inclusion complex formation in solid state as well as its properties, many assays could be used, such as scanning electronic microscopy (SEM), infrared spectroscopy (FTIR), thermal analysis (TA) and dissolution profile (DP).

SEM is a good option for assessing the morphological aspect of inclusion complex. The final form of the material can be related to the efficiency of the process. The CDs have a very characteristic form, in general amorphous, that changes with the complexation (PRALHAD; RAJENDRAKUMAR, 2004). In addition, the guests, normally in their crystalline form, are usually completely modified after inclusion complex. In general, the guests molecules are converted to an amorphous state (JUN et al., 2007).

Infrared spectroscopy is also a very common tool to evidence inclusion complex formation. In fact, the CD is capable of working as a “shield” for the guest, showing some alteration on the position and intensity of the characteristic bands of guest spectrum. Furthermore, the H bonds of CD with the guest molecule produce changes in the expected spectroscopic profile of the sample, providing additional evidences of complexation (CANNAVÀ et al., 2008; CRUPI et al., 2010; KAYACI; UYAR, 2011).

Thermal analyses are also useful for characterixation of inclusion complexes. Differential scanning calorimetry (DSC) provide consistent proofs of the influence of the CD on the guest molecules, based on its effect on the transition phase of the guest, such as melting or crystallization (MARQUES, 2010; MARQUES; HADGRAFT; KELLAWAY, 1990; PRALHAD; RAJENDRAKUMAR, 2004) The termogravimetry analysis (TGA), in turn, shows the thermal stability of the complexes produced in solid state (HUANG et al., 2016; JIAO; GOH; VALIYAVEETTIL, 2001; KAYACI; UYAR, 2011).

As already pointed out, one of the most noticeable effect of the complexation of hydrophobic guest molecules is in its water solubility properties. Therefore, determination of intrinsic solubility as well as the evaluation of dissolution profile are very powerful tests to study the inclusion complex phenomenon (SÁ-BARRETO et al., 2013).

Thus, CDs and their inclusion complexes have been used in many areas with several applications in industry, medicine and research. In the pharmaceutical and cosmetical field, CDs are already used to optimize the characteristics of several drugs with repercussion on their bioavailability. More specifically for topical administration purposes, besides their capacity of modifying the physicochemical characteristics of the drugs, CDs have been able to modulate drug permeation throught the skin, sometimes acting like a permeation enhancer and in other cases it can decrease the flux of drug through the skin layers (LOFTSSON; OLAFSSON, 1998).

1.3.4 Topical drug delivery and nanostructured lipid carriers

Strategies of drug delivery to epidermal layers are gaining prominence, since it presents many advantages over the systemic administration on numerous therapies, avoiding undesirable effects of the drugs which are distributed indiscriminately throughout the body. Besides that, the advantages of been less painful, non-invasive and comfortable make this kind of administration even more attractive (GELFUSO; CUNHA-FILHO; GRATIERI, 2016).

The main challenge for topical delivery on the epidermal layers is the surpass of the stratum corneum (SC). The SC is the most external and protective of the skin layers, due to its cell formation, composed of lipid and protein domains that limit the penetration of many molecules (MEHNERT; MÄDER, 2001).

Ideally, molecules for topical activity should present a low molecular weight (maximum of 500 Da); an intermediary partition coefficient making it relatively soluble in oil and water; and a highly potent action, capable of generating the desirable effect with a concentration as low as possible (preferable in a microgram per milliliter concentration range). The problem lays on the fact that even molecules with exceptional characteristics for SC penetration could not be suited for the topical administration, once a higher penetration can result in the drug arriving in more internal skin layers, such as the dermis, resulting in a systemic absortion, which causes undesirable effects. (GELFUSO; CUNHA-FILHO; GRATIERI, 2016)

Many strategies to overcome the SC barrier and also retaining the drug delivery in the skin layers have been developed in recent years, most of them involving the use of nanotechnology. A great variety of nanoparticles have been produced to control topical drug delivery. The main advantage of these systems is the potential of encapsulating the active, protecting against external agents and delivering it on specific regions, depending on the composition of the particles and their compatibility with the active molecules (KIM; RUTKA; CHAN, 2010). For topical administration, one of the strategies that have been proved to have

great results in the control of the permeation of actives in skin layers is the nanostructured lipid carriers (NLC) (CHAUDHARI, 2012).

NLC are a second generation of solid lipid nanoparticles formed by a solid lipid, in the exterior part of the particle and a liquid lipid, in the internal part (Figure 1.4). The liquid lipid is responsible to containing the active and because of its physical and chemical characteristics a numerous amount of molecules are capable to be encapsulated in the particle (TAMJIDI et al., 2013).

Figure 1.4 Basic chemical structure of cyclodextrin and conformation model (MONTENEGRO et al., 2016)

NLC composition is formed by biodegradable and biocompatible material which permits that in contact with the skin, at physiological temperature, occurs a formation of an occlusive film increasing skin hydration and drug penetration. An important characteristic of NLC is the permeation rout of those system. NLC has a preference for a non-classic permeation rout, through the hair follicle (HF). Normally, the permeation thorough the skin layers are made by two main routes, the transcellular and intercellular, however the permeation through the hair follicle, previously neglected, has gained enormous notoriety recently. (MONTENEGRO et al., 2016). Indeed, the HF rout become a very efficient way to deliver molecules in skin layers and with the help of systems such as NLC making possible a sustain release of the active, avoiding toxic effects (GELFUSO; CUNHA-FILHO; GRATIERI, 2016).

1.4 REFERENCES

ABARCA, R. L.; RODRÍGUEZ, F. J.; GUARDA, A.; GALOTTO, M. J.; BRUNA, J. E. Characterization of beta-cyclodextrin inclusion complexes containing an essential oil component. **Food Chemistry**, v. 196, p. 968–975, 2015.

ALTIERI, C.; SPERANZA, B.; DEL NOBILE, M. A.; SINIGAGLIA, M. Suitability of bifidobacteria and thymol as biopreservatives in extending the shelf life of fresh packed plaice fillets. **Journal of Applied Microbiology**, v. 99, n. 6, p. 1294–1302, 2005.

ANGELO, T.; PIRES, F. Q.; GELFUSO, G. M.; DA SILVA, J. K. R.; GRATIERI, T.; CUNHA-FILHO, M. S. S. Development and validation of a selective HPLC-UV method for thymol determination in skin permeation experiments. **Journal of Chromatography B: Analytical Technologies in the Biomedical and Life Sciences**, v. 1022, p. 81–86, 2016.

ARCHANA, P.; NAGESHWAR, B.; SATISH, B. In vivo radioprotective potential of thymol, a monoterpene phenol derivative of cymene. **Mutation research**, v. 726, n. 2, p. 136–45, 2011.

BANDI, N.; WEI, W.; ROBERTS, C. B.; KOTRA, L. P.; KOMPELLA, U. B. Preparation of budesonide- and indomethacin-hydroxypropyl-beta-cyclodextrin (HPBCD) complexes using a single-step, organic-solvent-free supercritical fluid process. **European journal of pharmaceutical sciences : official journal of the European Federation for Pharmaceutical Sciences**, v. 23, p. 159–168, 2004.

BASRA, M. K.; SHAHRUKH, M. The Burden of Skin Diseases. **Expert Reviews Pharmacoeconomics Outcomes**, v. 9, n. September, p. 271–283, 2005.

BETHANIS, K.; TZAMALIS, P.; TSORTEKI, F.; KOKKINOU, A.; CHRISTOFORIDES, E.; MENTZAFOS, D. Structural study of the inclusion compounds of thymol, carvacrol and eugenol in β-cyclodextrin by X-ray crystallography. **Journal of Inclusion Phenomena and Macrocyclic Chemistry**, v. 77, n. 1–4, p. 163–173, 2013.

BICKERS, D. R.; LIM, H. W.; MARGOLIS, D.; WEINSTOCK, M. A.; GOODMAN, C.; FAULKNER, E.; GOULD, C.; GEMMEN, E.; DALL, T. The burden of skin diseases: 2004. A joint project of the American Academy of Dermatology Association and the Society for Investigative Dermatology. **Journal of the American Academy of Dermatology**, v. 55, n. 3, p. 490–500, 2006.

BRAGA, P. C.; DAL SASSO, M.; CULICI, M.; BIANCHI, T.; BORDONI, L.; MARABINI, L. Anti-inflammatory activity of thymol: Inhibitory effect on the release of human neutrophil Elastase. **Pharmacology**, v. 77, n. 3, p. 130–136, 2006.

CALHAU, M. I. (Photographer). Parque das mangabeiras - Belo Horizonte. 2013. **Lippia origanoides - Verbanaceae**. Disponível em: <https://www.flickr.com/photos/ignezmotta/11254250556>. Acesso em: 18 jan. 2018.

CANNAVÀ, C.; CRUPI, V.; FICARRA, P.; GUARDO, M.; MAJOLINO, D.; STANCANELLI, R.; VENUTI, V. Physicochemical characterization of coumestrol/β-cyclodextrins inclusion complexes by UV-vis and FTIR-ATR spectroscopies. **Vibrational Spectroscopy**, v. 48, n. 2, p. 172–178, 2008.

CASTILLO, S.; PÉREZ-ALFONSO, C. O.; MARTÍNEZ-ROMERO, D.; GUILLÉN, F.; SERRANO, M.; VALERO, D. The essential oils thymol and carvacrol applied in the packing lines avoid lemon spoilage and maintain quality during storage. **Food Control**, v. 35, n. 1, p. 132–136, 2014.

CHANTASART, D.; PONGJANYAKUL, T.; HIGUCHI, W. I.; LI, S. K. Effects of oxygen-containing terpenes as skin permeation enhancers on the lipoidal pathways of human epidermal membrane. **Journal of Pharmaceutical s**, v. 98, n. 10, p. 3617–3632, 2009.

CHAPPELL, J. Biochemistry and Molecular Biology of the Isoprenoid Biosynthetic Pathway in Plants. **Annual Review of Plant Physiology and Plant Molecular Biology**, v. 46, n. 1, p. 521–547, 1995.

CHAUDHARI, Y. Nanoparticles - A paradigm for topical drug delivery. **Chronicles of Young Scientists**, v. 3, n. 1, p. 82, 2012.

CHEN, X.; CHEN, P. Determination of thymol content and related substances by RP-HPLC. **West China Journal of Pharmaceutical Sciences**, v. 2012–1, 2012.

CRINI, G. Review : A History of Cyclodextrins. **Chemical Reviews**, v. 114, n. 21, p. 10940–10975, 2014.

CRUPI, V.; MAJOLINO, D.; VENUTI, V.; GUELLA, G.; MANCINI, I.; ROSSI, B.; VERROCCHIO, P.; VILIANI, G.; STANCANELLI, R. Temperature effect on the vibrational dynamics of cyclodextrin inclusion complexes: Investigation by FTIR-ATR spectroscopy and numerical simulation. **Journal of Physical Chemistry A**, v. 114, n. 25, p. 6811–6817, 2010.

DAMASCENO, E. I. T.; SILVA, J. K. R.; ANDRADE, E. H. A.; SOUSA, P. J. C.; MAIA, J. G. S. Antioxidant capacity and larvicidal activity of essential oil and extracts from Lippia grandis. **Brazilian Journal of Pharmacognosy**, v. 21, n. 1, p. 78–85, 2011.

DE SOUZA, R. C.; VALARINI JÚNIOR, O.; PINHEIRO, K. H.; KLOSOSKI, S. J.; PIMENTEL, T. C.; CARDOZO FILHO, L.; BARÃO, C. E. Prebiotic green tea beverage added inclusion complexes of catechin and β-cyclodextrin: Physicochemical characteristics during storage. **LWT - Food Science and Technology**, v. 85, p. 212–217, 2017.

DEL VALLE, E. M. M. Cyclodextrins and their uses: A review. **Process Biochemistry**, v. 39, n. 9, p. 1033–1046, 2004.

FARAGE, M. A.; MILLER, K. W.; SHERMAN, S. N.; TSEVAT, J. Assessing quality of life in older adult patients with skin disorders. **Global journal of health science**, v. 4, n. 2, p. 119–31, 2012.

FERNANDES, L. P.; CANDIDO, R. C.; OLIVEIRA, W. P. Spray drying microencapsulation of Lippia sidoides extracts in carbohydrate blends. **Food and Bioproducts Processing**, v. 90, n. 3, p. 425–432, 2012.

FERNANDES, L. P.; OLIVEIRA, W. P.; SZTATISZ, J.; SZIL??GYI, I. M.; NOVAK, C. Solid state studies on molecular inclusions of lippia sidoides essential oil obtained by spray drying.

Journal of Thermal Analysis and Calorimetry, v. 95, n. 3, p. 855–863, 2009.

FREITAS, M. R. DE; ROLIM, L. A.; SOARES, M. F. D. L. R.; ROLIM-NETO, P. J.; ALBUQUERQUE, M. M. DE; SOARES-SOBRINHO, J. L. Inclusion complex of methyl-β-cyclodextrin and olanzapine as potential drug delivery system for schizophreniaCarbohydrate Polymers. **Carbohydrate polymers**, v. 89, n. 4, p. 1095-1100, 2012.

GELFUSO, G. M.; CUNHA-FILHO, M. S. S.; GRATIERI, T. Nanostructured lipid carriers for targeting drug delivery to the epidermal layer. **Ther. Deliv**, v. 7, n. 11, p. 735–737, 2016.

GREEN, L. The effect of skin conditions on patients' quality of life. **Nursing standard (Royal College of Nursing (Great Britain) : 1987)**, v. 25, n. 9, p. 48–55, 2010.

HAESELER, G.; MAUE, D.; GROSSKREUTZ, J.; BUFLER, J.; NENTWIG, B.; PIEPENBROCK, S.; DENGLER, R.; LEUWER, M. Voltage-dependent block of neuronal and skeletal muscle sodium channels by thymol and menthol. **European Journal of Anaesthesiology**, v. 19, n. 8, p. 571, 2002.

HAJIMEHDIPOOR, H.; SHEKARCHI, M.; KHANAVI, M.; ADIB, N.; AMRI, M. A validated high performance liquid chromatography method for the analysis of thymol and carvacrol in Thymus vulgaris L. volatile oil. **Pharmacognosy magazine**, v. 6, n. 23, p. 154–158, 2010.

HAY, R. J.; FULLER, L. C. The assessment of dermatological needs in resource-poor regions. **International Journal of Dermatology**, v. 50, n. 5, p. 552–557, 2011.

HAY, R. J.; JOHNS, N. E.; WILLIAMS, H. C.; BOLLIGER, I. W.; DELLAVALLE, R. P.; MARGOLIS, D. J.; MARKS, R.; NALDI, L.; WEINSTOCK, M. A.; WULF, S. K.; MICHAUD, C.; MURRAY, C. J. L.; NAGHAVI, M. The Global Burden of Skin Disease in 2010 : An Analysis of the Prevalence and Impact of Skin Conditions. **The Society Investigative Dermatology**, v. 134, p. 1527–1534, 2014.

HIDETOSHI, A.; MOTOYAMA, K.; IRIE, T. **Cyclodextrins in pharmaceutics, cosmetics and biomedicine: Current and future industrial applications**. Hoboken - USA: John Wiley & Sons, inc., 2011.

HUANG, Y.; ZU, Y.; ZHAO, X.; WU, M.; FENG, Z.; DENG, Y.; ZU, C.; WANG, L. Preparation of inclusion complex of apigenin-hydroxypropyl-β-cyclodextrin by using supercritical antisolvent process for dissolution and bioavailability enhancement. **International Journal of Pharmaceutics**, v. 511, n. 2, p. 921–930, 2016.

JENTSCH, H. F. R.; ECKERT, F. R.; ESCHRICH, K.; STRATUL, S. I.; KNEIST, S. Antibacterial action of Chlorhexidine/thymol containing varnishes in vitro and in vivo. **International Journal of Dental Hygiene**, v. 12, n. 3, p. 168–173, 2014.

JIAO, H.; GOH, S. H.; VALIYAVEETTIL, S. Inclusion complexes of poly(neopentyl glycol sebacate) with cyclodextrins. **Macromolecules**, v. 34, n. 23, p. 8138–8142, 2001.

JUN, S. W.; KIM, M.-S. S.; KIM, J.-S. S.; PARK, H. J.; LEE, S.; WOO, J.-S. S.; HWANG, S.-J. J. Preparation and characterization of simvastatin/hydroxypropyl-beta-cyclodextrin inclusion complex using supercritical antisolvent (SAS) process. **European journal of pharmaceutics**

and biopharmaceutics, v. 66, n. 3, p. 413–421, 2007.

JUNIOR, O. V.; DANTAS, J. H.; BARÃO, C. E.; ZANOELO, E. F.; CARDOZO-FILHO, L.; MORAES, F. F. Formation of inclusion compounds of (+)catechin with β-cyclodextrin in different complexation media: Spectral, thermal and antioxidant properties. **The Journal of Supercritical Fluids**, v. 121, p. 10–18, 2017.

KANG, S.-H.; KIM, Y.-S.; KIM, E.-K.; HWANG, J.-W.; JEONG, J.-H.; DONG, X.; LEE, J.-W.; MOON, S.-H.; JEON, B.-T.; PARK, P.-J. Anticancer Effect of Thymol on AGS Human Gastric Carcinoma Cells. **Journal of Microbiology and Biotechnology**, v. 26, n. 1, p. 28–37, 2016.

KAVOOSI, G.; DADFAR, S. M. M.; PURFARD, A. M. Mechanical, Physical, Antioxidant, and Antimicrobial Properties of Gelatin Films Incorporated with Thymol for Potential Use as Nano Wound Dressing. **Journal of Food Science**, v. 78, n. 2, 2013.

KAYACI, F.; UYAR, T. Solid inclusion complexes of vanillin with cyclodextrins: Their formation, characterization, and high-temperature stability. **Journal of Agricultural and Food Chemistry**, v. 59, n. 21, p. 11772–11778, 2011.

KHAZAEI, N.; ESMAIILI, M.; EMAM-DJOMEH, Z. Application of active edible coatings made from basil seed gum and thymol for quality maintenance of shrimp during cold storage. **Journal of the Science of Food and Agriculture**, v. 97, n. 6, p. 1837–1845, 2017.

KIM, B. Y. S.; RUTKA, J. T.; CHAN, W. C. W. Nanomedicine. **The New England Journal of Medicine**, v. 363, n. 25, p. 2434–2443, 2010.

KUMAR, D.; RAWAT, D. S. Synthesis and antioxidant activity of thymol and carvacrol based Schiff bases. **Bioorganic & Medicinal Chemistry Letters**, v. 23, n. 3, p. 641–645, 2013.

LAUTERBACH, A.; MÜLLER-GOYMANN, C. C. Comparison of rheological properties, follicular penetration, drug release, and permeation behavior of a novel topical drug delivery system and a conventional cream. **European Journal of Pharmaceutics and Biopharmaceutics**, v. 88, n. 3, p. 614–624, 2014.

LEE, S.-J.; UMANO, K.; SHIBAMOTO, T.; LEE, K.-G. Identification of volatile components in basil (Ocimum basilicum L.) and thyme leaves (Thymus vulgaris L.) and their antioxidant properties. **Food Chemistry**, v. 91, p. 131–137, 2005.

LI, K.; YUAN, J.; SU, W. Determination of Liquiritin, Naringin, Hesperidin, Thymol, Imperatorin, Honokiol, Isoimperatorin, and Magnolol in the Traditional Chinese Medicinal Preparation Huoxiang-zhengqi Liquid Using High-performance Liquid Chromatography. **Yakugaku Zasshi**, v. 126, n. 11, p. 1185–1190, 2006.

LOCCI, E.; LAI, S. M.; PIRAS, A.; MARONGIU, B.; LAI, A. C-13-CPMAS and H-1-NMR study of the inclusion complexes of beta-cyclodextrin with carvacrol, thymol, and eugenol prepared in supercritical carbon dioxide. **Chemistry & Biodiversity**, v. 1, n. 9, p. 1354–1366, 2004.

LOFTSSON, T.; HREINSDÓTTIR, D.; MÁSSON, M. Evaluation of cyclodextrin

solubilization of drugs. **International Journal of Pharmaceutics**, v. 302, n. 1–2, p. 18–28, 2005.

LOFTSSON, T.; OLAFSSON, J. H. Cyclodextrins: new drug delivery systems in dermatology. **International journal of dermatology**, v. 37, p. 241–246, 1998.

MARCHESE, A.; ORHAN, I. E.; DAGLIA, M.; BARBIERI, R.; LORENZO, A. DI; NABAVI, S. F.; GORTZI, O.; IZADI, M.; NABAVI, S. M. Antibacterial and antifungal activities of thymol: a brief review of the literature. **Food Chemistry**, v. 210, p. 402–414, 2016.

MARQUES, H. M. C. A review on cyclodextrin encapsulation of essential oils and volatiles. **Flavour and Fragrance Journal**, v. 25, n. 5, p. 313–326, 2010.

MARQUES, H. M. C.; HADGRAFT, J.; KELLAWAY, I. W. Studies of cyclodextrin inclusion complexes. I. The salbutamol-cyclodextrin complex as studied by phase solubility and DSC. **International Journal of Pharmaceutics**, v. 63, n. 3, p. 259–266, 1990.

MARRETO, R. N.; ALMEIDA, E. E. C. V; ALVES, P. B.; NICULAU, E. S.; NUNES, R. S.; MATOS, C. R. S.; ARAÚJO, A. A. S. Thermal analysis and gas chromatography coupled mass spectrometry analyses of hydroxypropyl-β-cyclodextrin inclusion complex containing Lippia gracilis essential oil. **Thermochimica Acta**, v. 475, n. 1–2, p. 53–58, 2008.

MEHNERT, W.; MÄDER, M. Solid lipid nanoparticles: production, characterization and applications. **Adv. Drug Del. Rev. Del Rev**, v. 47, p. 165–196, 2001.

MENDES, S. S.; BOMFIM, R. R.; JESUS, H. C. R.; ALVES, P. B.; BLANK, A. F.; ESTEVAM, C. S.; ANTONIOLLI, A. R.; THOMAZZI, S. M. Evaluation of the analgesic and anti-inflammatory effects of the essential oil of Lippia gracilis leaves. **Journal of Ethnopharmacology**, v. 129, n. 3, p. 391–397, 2010.

MOHAMMADI-SAMANI, S.; YOUSEFI, G.; MOHAMMADI, F.; AHMADI, F. Meloxicam transdermal delivery: Effect of eutectic point on the rate and extent of skin permeation. **Iranian Journal of Basic Medical Sciences**, v. 17, n. 2, p. 112–118, 2014.

MONTENEGRO, L.; LAI, F.; OFFERTA, A.; SARPIETRO, M. G.; MICICCHÈ, L.; MACCIONI, A. M.; VALENTI, D.; FADDA, A. M. From nanoemulsions to nanostructured lipid carriers: A relevant development in dermal delivery of drugs and cosmetics. **Journal of Drug Delivery Science and Technology**, v. 32, p. 100–112, 2016.

MULINACCI, N.; MELANI, F.; VINCIERI, F. F.; MAZZI, G.; ROMANI, A. 1H-NMR NOE and molecular modelling to characterize thymol and carvacrol β-cyclodextrin complexes. **International Journal of Pharmaceutics**, v. 128, n. 1–2, p. 81–88, 1996.

OLIVEIRA, D. R.; LEITÃO, G. G.; BIZZO, H. R.; LOPES, D.; ALVIANO, D. S.; ALVIANO, C. S.; LEITÃO, S. G. Chemical and antimicrobial analyses of essential oil of Lippia origanoides H.B.K. **Food Chemistry**, v. 101, n. 1, p. 236–240, 2006.

PASCUAL, M. E.; SLOWING, K.; CARRETERO, E.; SANCHEZ MATA, D.; VILLAR, A. Lippia: Traditional uses, chemistry and pharmacology: A review. **Journal of Ethnopharmacology**, v. 76, n. 3, p. 201–214, 2001.

PEREZ-VASQUEZ, A.; CAPELLA, S.; LINARES, E.; BYE, R.; ANGELES-LOPEZ, G.; MATA, R. Antimicrobial activity and chemical composition of the essential oil of Hofmeisteria schaffneri. **Journal of Pharmacy and Pharmacology**, v. 63, p. 579–586, 2011.

PRALHAD, T.; RAJENDRAKUMAR, K. Study of freeze-dried quercetin-cyclodextrin binary systems by DSC, FT-IR, X-ray diffraction and SEM analysis. **Journal of Pharmaceutical and Biomedical Analysis**, v. 34, n. 2, p. 333–339, 2004.

PRIESTLEY, C. M.; WILLIAMSON, E. M.; WAFFORD, K. A.; SATTELLE, D. B. Thymol, a constituent of thyme essential oil, is a positive allosteric modulator of human GABA A receptors and a homo-oligomeric GABA receptor from Drosophila melanogaster. **British Journal of Pharmacology**, v. 140, n. 8, p. 1363–1372, 2003.

RASSU, G.; NIEDDU, M.; BOSI, P.; TREVISI, P.; COLOMBO, M.; PRIORI, D.; MANCONI, P.; GIUNCHEDI, P.; GAVINI, E.; BOATTO, G. Encapsulation and modified-release of thymol from oral microparticles as adjuvant or substitute to current medications. **Phytomedicine**, v. 21, n. 12, p. 1627–1632, 2014.

RIELLA, K. R.; MARINHO, R. R.; SANTOS, J. S.; PEREIRA-FILHO, R. N.; CARDOSO, J. C.; ALBUQUERQUE-JUNIOR, R. L. C.; THOMAZZI, S. M. Anti-inflammatory and cicatrizing activities of thymol, a monoterpene of the essential oil from Lippia gracilis, in rodents. **Journal of Ethnopharmacology**, v. 143, n. 2, p. 656–663, 2012.

RUDRANGI, S. R. S.; TRIVEDI, V.; MITCHELL, J. C.; WICKS, S. R.; ALEXANDER, B. D. Preparation of olanzapine and methyl-β-cyclodextrin complexes using a single-step, organic solvent-free supercritical fluid process: An approach to enhance the solubility and dissolution properties. **International Journal of Pharmaceutics**, v. 494, n. 1, p. 408–416, 2015.

SÁ-BARRETO, L. C. L.; GUSTMANN, P. C.; GARCIA, F. S.; MAXIMIANO, F. P.; NOVACK, K. M.; CUNHA-FILHO, M. S. S. Modulated dissolution rate from the inclusion complex of antichagasic benznidazole and cyclodextrin using hydrophilic polymer. **Pharmaceutical Development and Technology**, v. 18, n. 5, p. 1035–1041, 2013.

SALÚSTIO, P. J.; CABRAL-MARQUES, H. M.; COSTA, P. C.; PINTO, J. F. Comparison of ibuprofen release from minitablets and capsules containing ibuprofen: β-Cyclodextrin complex. **European Journal of Pharmaceutics and Biopharmaceutics**, v. 78, n. 1, p. 58–66, 2011.

SALÚSTIO, P. J.; FEIO, G.; FIGUEIRINHAS, J. L.; PINTO, J. F.; CABRAL MARQUES, H. M. The influence of the preparation methods on the inclusion of model drugs in a β-cyclodextrin cavity. **European Journal of Pharmaceutics and Biopharmaceutics**, v. 71, n. 2, p. 377–386, 2009.

SAMBASEVAM, K. P.; MOHAMAD, S.; SARIH, N. M.; ISMAIL, N. A. Synthesis and characterization of the inclusion complex of β-cyclodextrin and azomethine. **International Journal of Molecular Sciences**, v. 14, n. 2, p. 3671–3682, 2013.

SANTOS, E. H.; KAMIMURA, J. A.; HILL, L. E.; GOMES, C. L. Characterization of carvacrol beta-cyclodextrin inclusion complexes as delivery systems for antibacterial and antioxidant applications. **LWT - Food Science and Technology**, v. 60, n. 1, p. 583–592, 2015.

SANTOS, M. R. V; MOREIRA, F. V.; FRAGA, B. P.; DE SOUSA, D. P.; BONJARDIM, L. R.; QUINTANS, L. J. Cardiovascular effects of monoterpenes: A review. **Brazilian Journal of Pharmacognosy**, v. 21, n. 4, p. 764–771, 2011.

SHAHIDI, F.; ZHONG, Y. Lipid oxidation and improving the oxidative stability. **Chemical Society reviews**, v. 39, n. 11, p. 4067–79, 2010.

SHIMODA, K.; KONDO, Y.; NISHIDA, T.; HAMADA, H.; NAKAJIMA, N.; HAMADA, H. Biotransformation of thymol, carvacrol, and eugenol by cultured cells of Eucalyptus perriniana. **Phytochemistry**, v. 67, n. 20, p. 2256–2261, 2006.

SILVA, L. A. D.; TEIXEIRA, F. V.; SERPA, R. C.; ESTEVES, N. L.; DOS SANTOS, R. R.; LIMA, E. M.; DA CUNHA-FILHO, M. S. S.; DE SOUZA ARAÚJO, A. A.; TAVEIRA, S. F.; MARRETO, R. N. Evaluation of carvedilol compatibility with lipid excipients for the development of lipid-based drug delivery systems. **Journal of Thermal Analysis and Calorimetry**, v. 123, n. 3, p. 2337–2344, 2016.

SOLINAS, V.; GESSA, C.; DELITALA, L. F. High-performance liquid chromatographic analysis of carvacrol and thymol in the essential oil of Thymus capitatus. **Journal of Chromatography A**, v. 219, n. 2, p. 332–337, 1981.

SWANSON, A.; CANTY, K. Common Pediatric Skin Conditions with Protracted Courses : A Therapeutic Update. v. 31, p. 239–249, 2013.

TAMJIDI, F.; SHAHEDI, M.; VARSHOSAZ, J.; NASIRPOUR, A. Nanostructured lipid carriers (NLC): A potential delivery system for bioactive food molecules. **Innovative Food Science and Emerging Technologies**, v. 19, p. 29–43, 2013.

TAN, X. C.; CHUA, K. H.; RAVISHANKAR RAM, M.; KUPPUSAMY, U. R. Monoterpenes: Novel insights into their biological effects and roles on glucose uptake and lipid metabolism in 3T3-L1 adipocytes. **Food Chemistry**, v. 196, p. 242–250, 2016.

TAO, F.; HILL, L. E.; PENG, Y.; GOMES, C. L. Synthesis and characterization of β-cyclodextrin inclusion complexes of thymol and thyme oil for antimicrobial delivery applications. **LWT - Food Science and Technology**, v. 59, n. 1, p. 247–255, 2014.

TASDEMIR, D.; KAISER, M.; DEMIRCI, F.; BASER, K. Essential oil of Turkish Origanum onites L. and its main components, carvacrol and thymol show potent antiprotozoal activity without cytotoxicity. **Planta Med**, v. 72, n. October 2016, p. 1006, 2006.

TELES, S.; ALBERTO, J.; MUNIZ, L.; OLIVEIRA, D.; MALHEIRO, R.; LUCCHESE, A. M.; SILVA, F. Lippia origanoides H . B . K . essential oil production , composition , and antioxidant activity under organic and mineral fertilization : Effect of harvest moment. **Industrial Crops & Products**, v. 60, p. 217–225, 2014.

YANISHLIEVA, N. V.; MARINOVA, E. M.; GORDON, M. H.; RANEVA, V. G. Antioxidant activity and mechanism of action of thymol and carvacrol in two lipid systems. **Food Chemistry**, v. 64, n. 1, p. 59–66, 1999.

CHAPTER 2- DEVELOPMENT AND VALIDATION OF A SELECTIVE HPLC-UV METHOD FOR THYMOL DETERMINATION IN SKIN PERMEATION EXPERIMENTS

Published in the Journal of Chromatography B – doi 10.1016/j.jchromb.201.04.011

This part of the work aim to develop and validate a novel, simple and selective analytical HPLC-UV method for thymol determination, which would give support for the development and evaluation of dermatological and cosmetic products containing this natural substance.

2.3 MATERIAL AND METHODS

2.3.1 Chemicals and reagents

Thymol (≥99.0%) was purchased from Sigma-Aldrich (Steinheim, Germany). Methanol and acetonitrile of HPLC grade were purchased from Tedia Brazil (Rio de Janeiro, Brazil). Porcine skin was obtained from a local abattoir (Bonasa Alimentos, São Sebastião, Brazil). Scotch book tape no. 845 (3M, St Paul, EUA) and cyanoacrylate glue Loctite (Henkel, Dublin, Ireland) were used to perform the differential tape stripping technique. All assays were performed using ultrapure Milli-Q water (Millipore, IllkirchGraffenstaden, France).

2.3.2 Samples preparation

A stock solution of thymol (500 µg/mL) was prepared by dissolving 5 mg of the drug in 10 mL of methanol. Standard solutions were prepared by suitable dilution of the stock solution in methanol.

Stratum corneum (SC) and hair follicle (HF) were separated from the remaining porcine skin (RS) following the differential tape stripping technique, as previously described (MATOS et al., 2015a; PATZELT et al., 2008). After the differential tape stripping, each skin layer sample was placed in individual closed glass flasks with 5 mL of methanol under stirring (300 rpm, overnight). The solvent was then filtered through a 0.22 µm membrane, producing skin extracts samples.

2.3.3 Chromatographic analysis

Thymol was quantified using a reversed-phase HPLC-UV method in a LC-20AD instrument (Shimadzu, Kyoto). UV detection was performed at 278 nm, oven temperature was 40 °C and the injection volume, 30 µL. Two columns were evaluated without the use of safe guards: (i) RP-C18 150 mm x 4.6 mm, 5 µm and (ii) RP-C18 300 mm x 3.9 mm, 10 µm. Different mobile phases and flow rates were tested to obtain the best peak resolution (Table 2.2).

2.3.4 Method Validation

The method was validated according to ICH guidelines (ICH, 2005), with respect to selectivity, robustness, linearity, limit of detection (LOD), limit of quantification (LOQ), precision and accuracy.

2.3.4.1 Seletivety

Standard thymol solution (7.5 µg/mL) was evaluated in the absence and in the presence of each skin extract to ensure that endogenous compounds present in the skin would not interfere on the drug peak. All assays were performed in six independent sources of each matrix. Results were analysed considering peak area and retention time (RT).

2.3.4.2 Robustness

Variations of ±5% in three selected analytical parameters (percentage of water in the mobile phase, flow rate and oven temperature) were implemented according to a factorial design (2^3), as presented in Table 2.1. All assays were performed in triplicate.

Table 2.1 Factorial design for robustness evaluation of the developed method for quantification of thymol.

Trial	Mobile phase (acetonitrile:water v/v)	Oven temperature (°C)	Flow rate (mL/min)
1	34:66	38	1.425
2	34:66	38	1.575
3	36:64	38	1.425
4	36:64	38	1.575
5	36:64	42	1.425
6	36:64	42	1.575
7	34:66	42	1.425
8	34:66	42	1.575

A prediction equation was proposed for each response (i.e., peak area and RT) using the analysis of multiple regressions step-wise. The model was validated by the analysis of variance (ANOVA) with a significance level of 0.05. All statistical calculations were performed using the software Design-Expert version 9.

2.3.4.3 Linearity

Three calibration curves were plotted in the range of 0.5 to –15 µg/mL of thymol and fitted using least squares linear regression. Angular coefficient significance and proportionality tests were evaluated based on the residual variance using student-t test ($\alpha = 0.05$). Response factors were calculated considering the ratio between peak area and analyte concentration. The residues were calculated based on the difference between theoretical and experimental values calculated from the calibration curve (PINHO et al., 2016).

2.3.4.4 Limit of detection (LOD) and limit of quantification (LOQ)

The LOD and LOQ were estimated considering the ratio of background noise and analytical signal (ICH, 2005). Thymol LOD and LOQ were calculated based on the calibration curve and calculated according to Eqs. (1) and (2) (ICH, 2005):

$$LOD = 3.3\ \sigma / S \qquad \text{(Eq. 1)}$$

$$LOQ = 10\ \sigma / S \qquad \text{(Eq. 2)}$$

where σ = the standard deviation of the response, S = the slope of the calibration curve.

2.3.4.5 Precision

Precision was evaluated in terms of repeatability and intermediate precision. Repeatability (intra-assay) was verified for three concentrations of thymol (0.5, 7.5 and 15.0 µg/mL) using three replicates of each. Intermediate precision was evaluated on two different days (inter-assay) using drug samples prepared by different analysts.

Results of precision were expressed as coefficient of variation (CV), calculated according to Eq (3):

CV = (standard deviation of the mean / mean) x 100 (Eq. 3).

2.3.4.6 Accuracy

Accuracy was reported as percent recovery of known added amounts of thymol from skin layers (GRATIERI et al., 2012). The method consisted of spiking the skin samples with three different known amounts of drug in methanol solution (0.5; 7.5 and 15.0 µg/mL). After solvent evaporation, skin samples were cut into small pieces and soaked in 5 mL of methanol. Samples were left overnight under constant stirring (300 rpm) at ambient temperature and then were filtered and analyzed using the HPLC-UV method described above. Thymol recovery was determined by calculating the ratio of the amount extracted from the skin samples to the amount added, determined by direct injection of spiking solution in the absence of skin. The experiments were performed in triplicate. Results of accuracy were calculated according to Eq (4):

Accuracy = (measured concentration / nominal concentration) x 100 (Eq. 4).

2.4. RESULTS AND DISCUSSION

2.4.1 Optimization of chromatographic conditions

To evaluate the most adequate method for thymol quantification in skin samples, the thymol solution (7.5 µg/mL) and SC, HF, RS extracts were injected separately. The chromatograms and RT of each sample were then analyzed. As none of the previously reported methods for thymol determination (CHEN; CHEN, 2012; HAJIMEHDIPOOR et al., 2010; LI; YUAN; SU, 2006; SOLINAS; GESSA; DELITALA, 1981) could separate thymol peak from skin interferences, a series of modifications were performed. Data presented in Table 2.2 summarize the analytical conditions executed.

Table 2.2 Variation in analytical conditions to develop HPLC-UV method fpr thymol quantification after skin permeation experiments.

Column	Trial	Mobile phase (v:v)	Flow rate (mL/min)	Thymol peak shape	Thymol RT (min)	Suitability
RP C_{18}; 150 × 4.6 mm; 5 μm	1	Methanol:water (70:30)	1.0	Tailing peak	6.471	Overleaping peaks
	2	Acetonitrile:methanol:water (25:50:25)	1.0	Tailing peak	3.720	Overleaping peaks
	3	Acetonitrile:methanol:water (15:50:35)	1.0	Tailing peak	6.326	Overleaping peaks
	4	Acetonitrile:methanol:water (10:50:40)	0.8	Tailing peak	11.251	Overleaping peaks
	5	Acetonitrile:water (60:40)	1.0	Tailing peak	4.805	Overleaping peaks
	6	Acetonitrile:water (30:70)	1.0	Tailing peak	6.254	Overleaping peaks
	7	Acetonitrile:water (25:75)	1.0	Suitable peak	8.286	Overleaping peaks
	8	Acetonitrile:water (25:75)	0.8	Suitable peak	10.384	Overleaping peaks
RP C_{18}; 300 × 3.9 mm; 10 μm	9	Acetonitrile:water (25:75)	1.0	Peak loss	–	–
	10	Acetonitrile:water (35:65)	1.0	Peak loss	–	–
	11	Acetonitrile:water (40:60)	1.0	Suitable peak	17.375	Overleaping peaks
	12	Acetonitrile:water (35:65)	1.5	Suitable peak	20.049	Suitable resolution
	13	Acetonitrile:water (35:65)	2.0	Suitable peak	15.912	Overleaping peaks

Initial tests (trials 1-6) were carried out with a RP-C18 (150 mm x× 4.6 mm, 5 μm) column, evaluating methanol:water, acetonitrile:methanol, acetonitrile:water and acetonitrile:methanol:water as possible mobile phases (Table 2.2). In all of these conditions the analyte peak overlapped the skin interferences peaks. Additionally, thymol peak showed high asymmetry, with tailing factors reaching 3.738, which may be caused by solvation and viscosity effect of the mobile phase (HAUN; TEUTENBERG; SCHMIDT, 2012). This undesired interaction between the analyte and the mobile phase can be solved adjusting the force of solvent system (MCNAIR; POLITE, 2007). In this way, some modifications in the flow rate were performed (trials 7 and 8), but drug and interferences peaks still eluted at the same RT.

A chromatographic column with more length (RP C18 : 300 × 3.9 mm; 10 μm) was tested in an attempt to improve peak resolution. Method trials number 9 and 10 resulted in peak loss, even following a 60 min running. This retention loss may have occurred due to the high content of water in mobile phase, which can fill column pores, turning them inaccessible to the analyte (WALTER; IRANETA; CAPPARELLA, 2005). Organic content in the mobile phase was thereby increased to 40% (v/v) (trial 11). However, drug RT was still in conflict with RT of matrices interferences. Hence, flow rate was adjusted in trials 12 and 13. Trial 12 moved thymol peak to a range out of skin interferences elution and was, therefore, selected for validation assays.

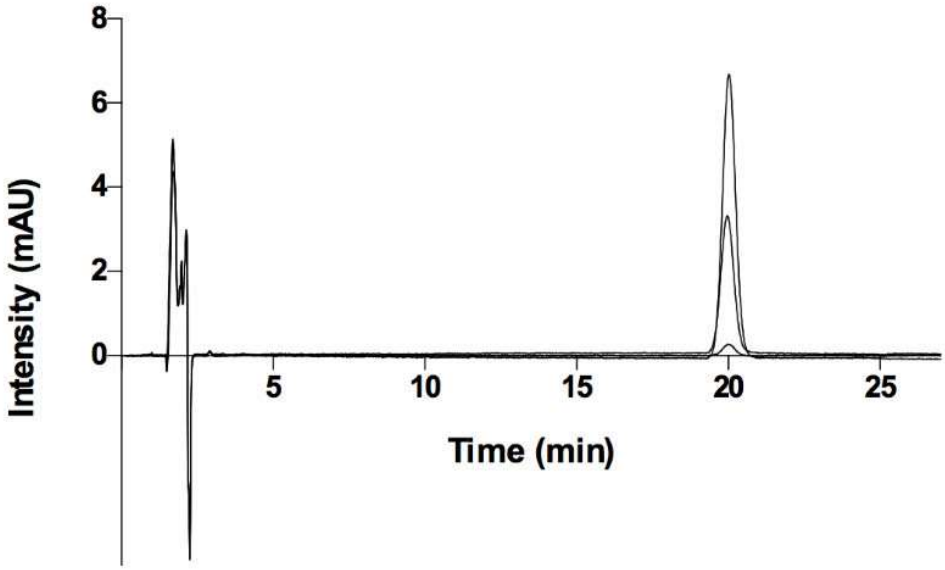

Figure 2.2 Representative overlaid HPLC chromatograms of thymol solutions at different concentrations (0.5; 7.5 and 15.0 µg/mL). RP-C18 column (300mm x 3.9 mm, 10µm), mobile phase of acetonitrile:water (35:65 v/v), flow rate of 1.5 mL/min, oven temperature at 40 °C, with injection volume of 30µL and detection at 278 nm.

Therefore, the selected method include the use a RP-C18 column (300 mm x× 3.9 mm, 10 µm), with an isocratic mobile phase of acetonitrile:water (35:65 v/v) at a flow rate of 1.5 mL/min. The oven temperature was set at 40 °C, the injection volume was of 30 µL and the detection occurred at 278 nm. Thymol RT was 20.5 min, with a running time of 27 min (Figure 2.2).

The efficiency of the method is expressed by the number of theoretical plates (N), which assumed the value of 9325 and is in agreement with FDA's established parameter of N > 2000 (FDA, 1994). The symmetry of the peak is established by the tailing factor (T), which was of 1.035, consistent with the limit of T < 1.5, defined by the USP (BONFILIO et al., 2012).

2.4.2 Validation

2.4.2.1 Selectivity

It is observed in Figure 2.3 that most contaminants from the skin fractions eluted over the first 10 min of running, with some peaks eluting until 18 min. For the SC fraction, an additional contamination peak was noted at 24 min. Thymol peak eluted after 20 min, free of any interference from solvent or skin components.

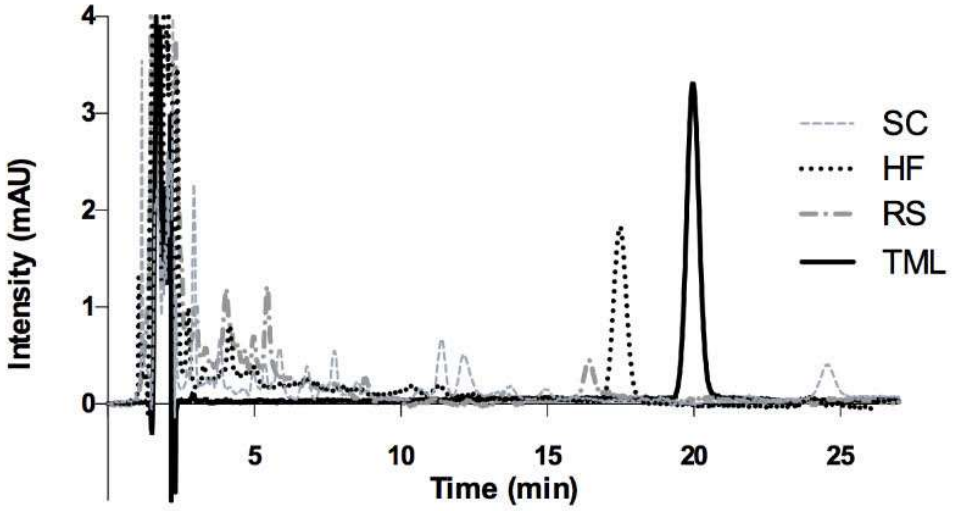

Figure 2.3 Representative overlaid HPLC chromatograms of SC = stratum corneum; HF = hair follicle; RS = remaining skin and TML = thymol . RP-C18 column (300mm x 3.9 mm, 10µm), mobile phase of acetonitrile:water (35:65 v/v), flow rate of 1.5 mL/min, oven temperature at 40 °C, with injection volume of 30µL and detection at 278 nm.

Figure 2.4 shows skin matrix interferents did not alter drug RT. Likewise, thymol peak areas were not changed in the presence of the biological matrix, confirming the method selectivity.

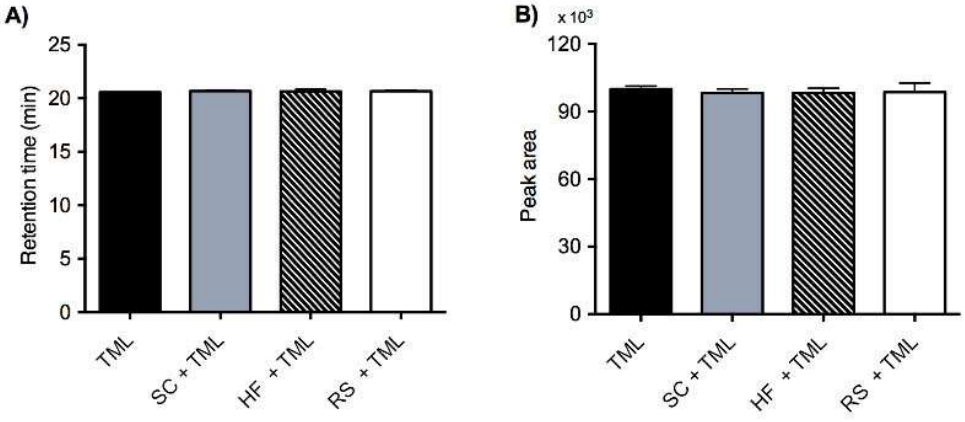

Figure 2.4 Selectivity of the method in quantification of thymol (7.5 µg/mL) alone and added to skin layer extracts. Analysis in terms of (A) retention times and (B) peak areas. All assays performed with six independent sources of each sample. SC = stratum corneum; HF = hair follicle; RS = remain skin.

2.4.2.2 Robustness

A predictive model was constructed to elucidate how each response (thymol peak area and RT) behaves according to variations in analytical parameters and their mutual interactions (Eqs. (5) and (6)).

$$\text{Area} = +\ 2.3\ x10^5 - 447.8\ WC + 121.5\ T - 65{,}452.2\ FR \quad \text{(Eq. 5)}$$

$$RT\ (min) = -\ 238.7 + 4.5\ WC - 0.3\ T - 98.4\ FR - 1.7WCT \quad \text{(Eq. 6)},$$

where WC is the water content (% v/v); T is the oven temperature (°C); and FR is flow rate (mL/min).

The proposed predictive model for peak area had a high statistical significance ($p < 0.0001$) with R^2 of 0.9864, which allowed for predictions within the design space with a high degree of accuracy. No significant interaction was identified among the three studied factors. Considering the variation margins studied, only the flow rate caused important changes in the peak areas of thymol. Lower flow rates produced higher molecular diffusion time in the column, resulting in broaden peaks (KAZAKEVICH, 2007). Indeed, the response surface graph presented in Figure 2.5 clearly shows the increase in flow rate, even within narrow margins, reduced the values of thymol peak area (negative coefficient of the equation). Variations in temperature and water percentage in the mobile phase within studied ranges did not generate significant changes in peak areas of the chromatograms assigned to the analyte.

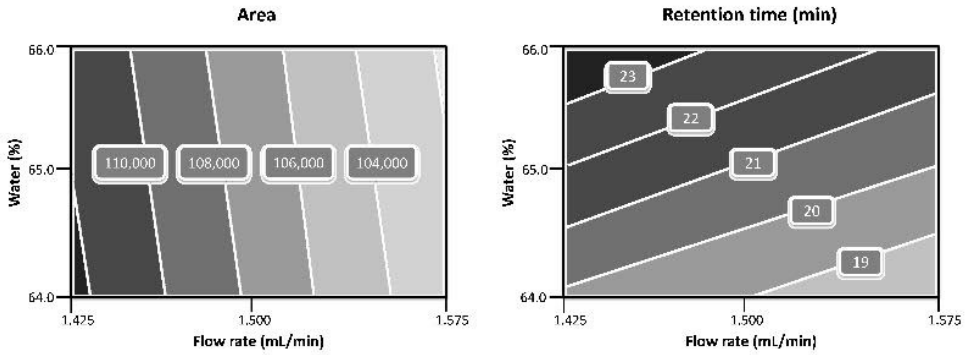

Figure 2.5 Response surfaces for thymol peak area and retention time in robustness assay.

In case of RT, the proposed predictive model ($p < 0.0001$) also presented a high predictive ability ($R^2 = 0.9894$). The model is composed by the three factors, also including the interaction between water content and flow rate. For this response, all terms of equation were statistically significant, and variations in flow rate, once again, produced the most pronounced

changes in thymol RT. This result was expected, since the peak position peak is strongly influenced by the flow rate (MCNAIR; POLITE, 2007).

Variations of the column temperature also had an impact on the drug RT due to the viscosity changes on the mobile fase; however, such impact was considerably less extreme compared to that produced by flow rate variations (equation coefficients ∞ 300-fold lower).

The polarity of the mobile phase, as might be expected, also influenced the drug RT. Small changes in water percentage in the mobile phase increased polarity and shifted the analyte peak (MCNAIR; POLITE, 2007).

Combination of deliberate variations in water content or in the flow rate changed the RT (Figure 2.5). The combination of these factors was especially relevant for such response.

In general, the developed analytical method presented good sensitivity. Hence, oscillations found in area response due the studied factors did not bring great impact on the analytical method sensitivity. Regarding RT, analyzed variations in chromatographic conditions produced changes not only for the analyte peak but also for the interferents. As interferents and analyte peaks shifts may not always be proportional, in some conditions method selectivity may be compromised. Thus, the necessity of a strict control over the flow rate is evident. Equipment preventive maintenance should be sufficient to ensure accurate operation of the pumps, avoiding oscillations on flow rate and mobile phase mixture (MCNAIR; POLITE, 2007).

2.4.2.3 Linearity

Linear regression of the calibration curve obtained the following equation: y = 13,395x − 502.1. The high numerical value of slope (13,395) indicates a good methodological sensitivity. This result was expected based on the wide concentration range proposed (0.5–15 μg/mL). Student's t-test showed the slope was different from zero, with a confidence interval from 13.1 to 13.7.

The independent term (−502.1) can be attributed to the systematic error of the method, as demonstrated by the proportionality test that shows a confidence interval between −2,894 and 1890.

The results of least squares linear regression analysis showed that the correlation coefficients of all the standard curves were ≥0.999, which complies with all regulatory requirements for this parameter (SHABIR, 2004).

Calculation of residues showed a random data distribution with equivalent numbers of

positive and negative residues, with no tendency. The response factors calculated from each of the curve points were very similar among each other and close to the numerical value of the slope. Coefficient of variation of the response factors was around 2.5%, within the acceptable limit of 5%, ratifying the linearity of the method (MATOS et al., 2015b; SHABIR, 2004).

2.4.2.4 Limit of detection and limit of quantification

The obtained LOD and LOQ values were, respectively 0.05 µg/mL and 0.14 µg/mL. Such values may be sufficient for determination of drug permeation kinetics profile into the skin from initial sampling points.

2.4.2.5 Precision

The proposed method was quite resistant to the variables proposed, with coefficient of variation values lower than 2% (Table 2.3). This data is below the limits of 5% for bioanalytical methods by a large margin, and also meets the recommended limits for methods employed in assays of raw materials and dosage forms establishing a maximum coefficient of variation of 2%.

Table 2.3 Results of precision tests for determination of thymol in standard solutions.

Thymol TC[a] (µg/mL)	Repeatability		Intermediate precision	
	Thymol MC[a] (µg/mL)	CV[a] (%)	Thymol MC[a] (µg/mL)	CV[a] (%)
0.50	0.49	0.73	0.52	1.35
7.50	7.44	0.38	7.56	0.83
15.00	15.49	0.32	15.40	0.99

[a] TC = theoretical concentration; MC = measured concentration; CV = coefficient of variation.

2.4.2.6 Accuracy

Table 2.4 summarizes the accuracy found for recovered thymol, with values higher than 90% for all drug concentrations and biological matrices evaluated. Thymol recovery achieved in HF matrix was close to 100%. Such results eliminate the need of using a correction factor during the permeation experiments, as according to the literature drug recovery rates from skin above 70% can be acceptable (CAMPOS; PRAÇA; BENTLEY, 2015; DE PAULA; MARTINS; BENTLEY, 2008; VÁVROVÁ et al., 2007).

Table 2.4 Results of precision tests for determination of thymol recovered from skin layers.

	Stratum corneum			Hair follicle			Remaining skin		
Thymol TC[a] (μg/mL)	Thymol MC[a] (μg/mL)	CV[a] (%)	Recovery (%)	Thymol MC[a] (μg/mL)	CV[a] (%)	Recovery (%)	Thymol MC[a] (μg/mL)	CV[a] (%)	Recovery (%)
0.5	0.46	5.17	92.00	0.50	8.37	100.00	0.49	8.34	98.00
7.5	6.95	8.13	92.67	7.43	3.85	99.07	7.32	3.16	97.60
15.0	14.42	3.37	96.13	15.04	2.73	100.27	14.82	4.56	98.80

[a] TC = theoretical concentration; MC = measured concentration; CV = coefficient of variation.

Coefficients of variation found for this validation parameter were below 10%, meeting the set limits by international health authorities, which is of 15% in case of bioanalytical methods (BANSAL; DESTEFANO, 2007; SHAH et al., 2000).

2.5 CONCLUSION

Biological matrices are complex and present two major analytical challenges: the drug recovery from the matrix and drug separation from interferences during the analytical procedure. The diverse nature of contaminants found in the different skin layers is an additional factor of difficulty. The developed analytical method circumvented all these challenges. It was selective for thymol and presented recovery rates higher than 90% using a simple HPLC-UV apparatus. The validation showed the method might be useful for *in vitro* skin permeation studies of topical dermatological or cosmetic products containing thymol.

2.6 ACKNOWLEDGMENTS

This research was supported by Brazilian agencies CNPq, CAPES and FAP-DF. The authors would also like to thank “Bonasa Alimentos” for gently providing porcine skin.

2.7 REFERENCES

ABBASZADEH, S.; SHARIFZADEH, A.; SHOKRI, H.; KHOSRAVI, A. R.; ABBASZADEH, A. Antifungal efficacy of thymol, carvacrol, eugenol and menthol as alternative agents to control the growth of food-relevant fungi. **Journal de mycologie médicale**, v. 24, n. 2, p. e51–e56, 2014.

AESCHBACH, R.; LÖLIGER, J.; SCOTT, B. C.; MURCIA, A.; BUTLER, J.; HALLIWELL, B.; ARUOMA, O. I. Antioxidant actions of thymol, carvacrol, 6-gingerol, zingerone and hydroxytyrosol. **Food and Chemical Toxicology**, v. 32, n. 1, p. 31–36, 1994.

ARAVENA, G.; GARCÍA, O.; MUÑOZ, O.; PÉREZ-CORREA, J. R.; PARADA, J. The impact of cooking and delivery modes of thymol and carvacrol on retention and bioaccessibility in starchy foods. **Food Chemistry**, v. 196, p. 848–52, 2016.

BAKKALI, F.; AVERBECK, S.; AVERBECK, D.; IDAOMAR, M. Biological effects of essential oils - A review. **Food and Chemical Toxicology**, v. 46, n. 2, p. 446–475, 2008.

BANSAL, S.; DESTEFANO, A. Key Elements of Bioanalytical Method Validation for Small Molecules. **The AAPS journal**, v. 9, n. 1, p. E109–E114, 2007.

BASCH, E.; BASCH, E. Thyme (Thymus vulgaris L .), Thymol Thyme (Thymus vulgaris L .), Thymol. **Journal of Herbal Pharmacotherapy: February 2004**, v. 4, n. August, p. 49–67, 2015.

BONFILIO, R.; CAZEDEY, E. C. L.; ARAÚJO, M. B. DE; NUNES SALGADO, H. R. Analytical Validation of Quantitative High-Performance Liquid Chromatographic Methods in Pharmaceutical Analysis: A Practical Approach. **Critical Reviews in Analytical Chemistry**, v. 42, n. 1, p. 87–100, 2012.

BORGHETI-CARDOSO, L. N.; ÂNGELO, T.; GELFUSO, G. M.; LOPEZ, R. F. V; GRATIERI, T. Topical and transdermal delivery of drug-loaded nano/microsystems with application of physical enhancement techniques. **Current Drug Targets**, n. [Epub ahead of print], 2015.

CAMPOS, P. M.; PRAÇA, F. S. G.; BENTLEY, M. V. L. B. Quantification of lipoic acid from skin samples by HPLC using ultraviolet, electrochemical and evaporative light scattering detectors. **Journal of Chromatography B**, n. In Press, 2015.

CHEN, X.; CHEN, P. Determination of thymol content and related substances by RP-HPLC. **West China Journal of Pharmaceutical Sciences**, v. 2012–1, 2012.

CROCKER, H. R. Thymol as a Remedy in Skin-Diseases. **British medical journal**, v. 1, n. 894, p. 225–6, 1878.

DAMASCENO, E. I. T.; SILVA, J. K. R.; ANDRADE, E. H. A.; SOUSA, P. J. C.; MAIA, J. G. S. Antioxidant capacity and larvicidal activity of essential oil and extracts from Lippia grandis. **Brazilian Journal of Pharmacognosy**, v. 21, n. 1, p. 78–85, 2011.

DE PAULA, D.; MARTINS, C. A.; BENTLEY, M. V. L. B. Development and validation of

HPLC method for imiquimod determination in skin penetration studies. **Biomedical Chromatography**, v. 22, n. 12, p. 1416–1423, 2008.

FDA. **Reviewer Guidance - Validation of chromatographic methodsCDER. Center for Drug Evaluation and Research**Rockville, United States of America, 1994.

GOODNER, K. L.; MAHATTANATAWEE, K.; PLOTTO, A.; SOTOMAYOR, J. A.; JORDAN, M. J. Aromatic profiles of Thymus hyemalis and Spanish T. vulgaris essential oils by GC-MS/GC-O. **Industrial Crops and Products**, v. 24, n. 3, p. 264–268, 2006.

GRATIERI, T.; WAGNER, B.; KALARIA, D.; ERNST, B.; KALIA, Y. N. Development and validation of a HPAE-PAD method for the quantification of CGP69669A, a sialyl Lewis x mimetic, in skin permeation studies. **Biomedical Chromatography**, v. 26, n. 4, p. 507–511, 2012.

HAJIMEHDIPOOR, H.; SHEKARCHI, M.; KHANAVI, M.; ADIB, N.; AMRI, M. A validated high performance liquid chromatography method for the analysis of thymol and carvacrol in Thymus vulgaris L. volatile oil. **Pharmacognosy magazine**, v. 6, n. 23, p. 154–158, 2010.

HAUN, J.; TEUTENBERG, T.; SCHMIDT, T. C. Influence of temperature on peak shape and solvent compatibility: Implications for two-dimensional liquid chromatography. **Journal of Separation Science**, v. 35, n. 14, p. 1723–1730, 2012.

HAY, I. C.; JAMIESON, M.; ORMEROD, A. D. Randomized Trial of Aromatherapy. **Archives of Dermatology**, v. 134, n. 11, p. 1349–1352, 1998.

ICH. **Harmonised Tripartite Guideline - Validation of Analytical Procedures: Text and Methodology - Q2 (R1)**Geneva, Switzerland, 2005.

KAZAKEVICH, Y. V. HPLC Theory. In: AHUJA, S.; RASMUSSEN, H. (Eds.). . **Separation Science and Technology**. [s.l.] Academic Press, 2007. v. 8p. 13–44.

KORDALI, S.; CAKIR, A.; OZER, H.; CAKMAKCI, R.; KESDEK, M.; METE, E. Antifungal, phytotoxic and insecticidal properties of essential oil isolated from Turkish Origanum acutidens and its three components, carvacrol, thymol and p-cymene. **Bioresource Technology**, v. 99, n. 18, p. 8788–8795, 2008.

LI, K.; YUAN, J.; SU, W. Determination of Liquiritin, Naringin, Hesperidin, Thymol, Imperatorin, Honokiol, Isoimperatorin, and Magnolol in the Traditional Chinese Medicinal Preparation Huoxiang-zhengqi Liquid Using High-performance Liquid Chromatography. **Yakugaku Zasshi**, v. 126, n. 11, p. 1185–1190, 2006.

LIOLIOS, C. C.; GORTZI, O.; LALAS, S.; TSAKNIS, J.; CHINOU, I. Liposomal incorporation of carvacrol and thymol isolated from the essential oil of Origanum dictamnus L. and in vitro antimicrobial activity. **Food Chemistry**, v. 112, n. 1, p. 77–83, 2009.

MASTROMATTEO, M.; MASTROMATTEO, M.; CONTE, A.; DEL NOBILE, M. A. Advances in controlled release devices for food packaging applications. **Trends in Food Science & Technology**, v. 21, n. 12, p. 591–598, 2010.

MATOS, B. N.; OLIVEIRA, P. M. DE; REIS, T. A.; GRATIERI, T.; CUNHA-FILHO, M.; GELFUSO, G. M. Development and Validation of a Simple and Selective Analytical HPLC Method for the Quantification of Oxaliplatin. **Journal of Chemistry**, v. 2015, n. http://dx.doi.org/10.1155/2015/812701, p. 1–6, 2015a.

MATOS, B. N.; REIS, T. A.; GRATIERI, T.; GELFUSO, G. M. Chitosan nanoparticles for targeting and sustaining minoxidil sulphate delivery to hair follicles. **International Journal of Biological Macromolecules**, v. 75, p. 225–229, 2015b.

MCNAIR, H.; POLITE, L. N. Troubleshooting in High Performance Liquid Chromatography. In: AHUJA, S.; RASMUSSEN, H. (Eds.). . **Separation Science and Technology**. [s.l.] Academic Press, 2007. v. 8p. 459–477.

NOVY, P.; DAVIDOVA, H.; SUQUED, C. Composition and Antimicrobial Activity of Euphrasia rostkoviana Hayne Essen...: Discovery Service for Endeavour College of Natural Health Library. **Evidance-Based Complimentary & Alternative Medicine**, v. 2015, p. 1–5, 2015.

OLIVEIRA, D. R.; LEITÃO, G. G.; BIZZO, H. R.; LOPES, D.; ALVIANO, D. S.; ALVIANO, C. S.; LEITÃO, S. G. Chemical and antimicrobial analyses of essential oil of Lippia origanoides H.B.K. **Food Chemistry**, v. 101, n. 1, p. 236–240, 2006.

PATZELT, A.; RICHTER, H.; BUETTEMEYER, R.; HUBER, H. J. R.; BLUME-PEYTAVI, U.; STERRY, W.; LADEMANN, J. Differential stripping demonstrates a significant reduction of the hair follicle reservoir in vitro compared to in vivo. **European Journal of Pharmaceutics and Biopharmaceutics**, v. 70, n. 1, p. 234–238, 2008.

PINHO, L. A. G.; SÁ-BARRETO, L. C.; INFANTE, C. M. C.; CUNHA-FILHO, M. S. S. Simultaneous Determination of Benznidazole and Itraconazole using Spectrophotometry Applied to the Analysis of Mixture: A Tool for Quality Control in the Development of Formulations. **Latin American Journal of Pharmacy**, v. 159, p. 48–52, 2016.

RIELLA, K. R.; MARINHO, R. R.; SANTOS, J. S.; PEREIRA-FILHO, R. N.; CARDOSO, J. C.; ALBUQUERQUE-JUNIOR, R. L. C.; THOMAZZI, S. M. Anti-inflammatory and cicatrizing activities of thymol, a monoterpene of the essential oil from Lippia gracilis, in rodents. **Journal of Ethnopharmacology**, v. 143, n. 2, p. 656–663, 2012.

SHABIR, B. Y. G. Step-by-step analytical methods validation and protocol in the quality system compliance industry. **Journal of Validation Technology**, v. 10, p. 210–218, 2004.

SHAH, V. P.; MIDHA, K. K.; FINDLAY, J. W.; HILL, H. M.; HULSE, J. D.; MCGILVERAY, I. J.; MCKAY, G.; MILLER, K. J.; PATNAIK, R. N.; POWELL, M. L.; TONELLI, A.; VISWANATHAN, C. T.; YACOBI, A. Bioanalytical method validation - a revisit with a decade of progress. **Pharmaceutical Research**, v. 17, n. 12, p. 1551–1557, 2000.

SOLINAS, V.; GESSA, C.; DELITALA, L. F. High-performance liquid chromatographic analysis of carvacrol and thymol in the essential oil of Thymus capitatus. **Journal of Chromatography A**, v. 219, n. 2, p. 332–337, 1981.

VÁVROVÁ, K.; LORENCOVÁ, K.; KLIMENTOVÁ, J.; NOVOTNÝ, J.; HRABÁLEK, A.

HPLC method for determination of in vitro delivery through and into porcine skin of adefovir (PMEA). **Journal of Chromatography B**, v. 853, n. 1–2, p. 198–203, 2007.

WALTER, T. H.; IRANETA, P.; CAPPARELLA, M. Mechanism of retention loss when C8 and C18 HPLC columns are used with highly aqueous mobile phases. **Journal of Chromatography A**, v. 1075, p. 177–183, 2005.

WATTANASATCHA, A.; RENGPIPAT, S.; WANICHWECHARUNGRUANG, S. Thymol nanospheres as an effective anti-bacterial agent. **International Journal of Pharmaceutics**, v. 434, n. 1–2, p. 360–365, 2012.

WECHSLER, J. B.; HSU, C. L.; BRYCE, P. J. IgE-mediated mast cell responses are inhibited by thymol-mediated, activation-induced cell death in skin inflammation. **Journal of Allergy and Clinical Immunology**, v. 133, n. 6, p. 1735–1743, 2014.

WILSON, J. W. Paronychia and Onycholysis, Etiology and Therapy. **Archives of Dermatology**, v. 92, n. 6, p. 726, 1965.

ZAMUREENKO, V. A.; KLYUEV, N. A.; BOCHAROV, B. V.; KABANOV, V. S.; ZAKHAROV, A. M. An investigation of the component composition of the essential oil of Monarda fistulosa. **Chemistry of Natural Compounds**, v. 25, n. 5, p. 549–551, 1989.

CHAPTER 3- USE OF MIXTURE DESIGN IN DRUG-EXCIPIENT COMPATIBILITY DETERMINATIONS: THYMOL NANOPARTICLES CASE STUDY

Published in the Journal of Pharmaceutical and Biomedical Analysis – doi 10.1016/j.jpba.2017.01.037

This part of the work describes an experimental mixture design associated with thermal and spectroscopic analyzes as a tool to define each formulation component contribution on TML stability. The aim is to determine possible interactions between components and to evaluate risks of associated excipients. Despite guiding formulation development, this paper suggests a new experimental approach for compatibility studies.

3.4 MATERIAL AND METHODS

3.4.1 Materials

TML (Lot SZBF0370V, purity ≥ 99%) and sodium taurodeoxycholate (TAU, purity ≥ 95%) were purchased from Sigma-Aldrich (Steinheim, Germany). Stearic acid (SA) was purchased from Dinâmica Química Contemporânea Ltda (São Paulo, Brazil). Soybean Lecithin (LC) was purchased from Lipoid (Ludwigshafen, Germany). Polysorbate 80 (P80) was purchased from Merck (Darmstadt, Germany).

3.4.2 Experimental mixture design

A drug-excipient compatibility study with TML and selected excipients commonly used to prepare nanostructured carriers was conducted following a simplex centroid mixture design with three components, without constraints (ERIKSSON; JOHANSSON; WIKSTROM, 1998). In the design A, fatty acid SA and phospholipid LC were mixed with the anionic surfactant TAU. In the design B, TAU was replaced by the nonionic surfactant P80. Mixtures were prepared in a mortar containing 50% (w/w) of TML and 50% (w/w) of other components according to the mixture design (Table 3.1). Experiments were performed randomly. The responses obtained from thermal analysis (TML melting peak variation, TML evaporation peak variation and excipient decomposition peak variation) and spectroscopy assays (sample stability based on correlation coefficient of spectra) were analyzed using the software Design Expert 8.0 (Stat-Ease, USA). The possible models were analyzed using ANOVA one-way. The

best fitting model was selected for each response based on *p-value* and a predictive equation containing only significant terms was built from stepwise multiple regression analysis.

Table 3.1 Mixtures composition studied according to the simplex centroid mixture design. TML: thymol; LC: soybean lecithin; P80: polysorbate 80; SA: stearic acid; TAU: sodium taurodeoxycholate.

Mixture	TML (%, w/w)	SA (%, w/w)	LC (%, w/w)	TAU (*design A*) or P80 (*design B*) (%, w/w)
1	50	50.0	-	-
2	50	-	50.0	-
3	50	-	-	50.0
4	50	25.0	25.0	-
5	50	25.0	-	25.0
6	50	-	25.0	25.0
7	50	16.7	16.7	16.7

3.4.3 Thermal analysis

Differential thermal analysis (DTA) and thermogravimetric analyses (TGA) were performed simultaneously using a Shimadzu® DTG-60 series under nitrogen controlled atmosphere with flow of 50 $mL \cdot min^{-1}$. Samples of approximately 3 mg were analysed in a platinum pan in a heating range of 25 ºC - 450 ºC using a heating rate of 10 ºC min^{-1}. TML melting peak was calculated from DTA data and T_{peak} for TML evaporation and excipient decomposition were obtained from the first derivative of mass loss curves of TGA. Thermal measurements were determined using the TA-60 Shimadzu® software.

3.4.4 Fourier Transform Infrared Spectroscopy (FTIR)

The FTIR analyses were performed using a Varian 640-IR FTIR spectrometer (Varian Inc., Brazil). The spectra were recorded between 650 cm^{-1} and 4000 cm^{-1} using an ATR imaging accessory. Individual compounds and mixtures of TML and excipients were evaluated before and after a thermal stressing (heating samples until 80 ºC). The resulting spectra were analyzed considering the correlation coefficient (r) between samples based on the bands corresponding

to the functional groups of the drug and the excipients using the Essential FTIR software (Operant LLC, USA).

3.5 RESULTS AND DISCUSSION

3.5.1 Thermal analysis

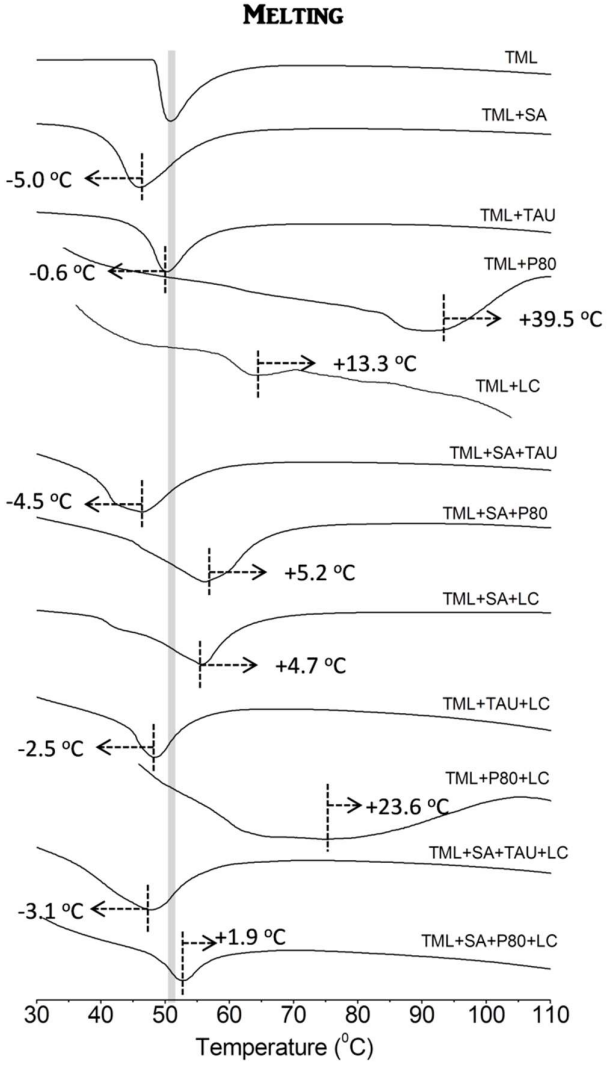

Figure 3.1. DTA curves of thymol (TML) and its mixtures according to the mixture designs. TML melting peak is shaded and the shifts on melting temperature are indicated in each mixture. LC: soybean lecithin; P80: polysorbate 80; SA: stearic acid; TAU: sodium taurodeoxycholate.

In simultaneous DTA-TGA analysis the melting of TML occurred at 50.9 °C with an associated endotherm of 923 $J \cdot g^{-1}$, followed by evaporation of the drug in the range of 67 °C – 144 °C (T_{peak} = 139.9 °C). In the mixtures with selected excipients, the correspondent thermal events of each component plus the decomposition of excipients, which occurs at temperatures above 200 °C, could be observed. Both TML characteristic thermal events, as well as excipients decomposition were used as thermal control parameters to study the compatibility among compounds.

There is a noticeable thermal interaction in almost all studied systems, with drug melting peak shifts from -5 °C to +39.5 °C regarding the expected temperature of 50.9 °C. In contrast, in TML+TAU binary mixture the expected melting peak temperature was maintained (Figure 3.1).

In mixtures containing SA (Figure 3.1), an overlap of TML and fatty acid melting was observed to a temperature lower than expected, which suggests the formation of an eutectic mixture (KANG; JUN; MANI, 2001; ZHANG et al., 2014). Both LC and P80 caused a pronounced displacement of TML melting peak to higher temperatures. In the case of LC, a marked reduction in the expected enthalpy was further observed, probably following drug solubilization. Noteworthy, TML melting was increased in more than 20°C in the ternary system containing LC and P80 (Figure 3.1).

Table 3.2. Fitting model, p value, F value, predictive equation and regression coefficient (R^2) for each response of the mixtures designs (A and B). LC: soybean lecithin; P80: polysorbate 80; SA: stearic acid; TAU: sodium taurodeoxycholate; TML: thymol.

Response		Model	P value	F value	Predictive equation	R^2
Melting	A	Quadratic	*0.0037*	*58.34*	ΔT_{peak} (°C) = − 0.11SA% + 0.27LC% − 0.03TAU% − 0.02LC%.TAU%	0.96
	B	Linear	*0.0435*	*7.59*	ΔT_{peak} (°C) = − 0.20SA% + 0.24LC% + 0.67P80%	0.84
Evaporation	A	Linear	*0.0428*	*7.66*	ΔT_{peak} (°C) = + 0.08SA% + 0.17LC% − 0.29TAU%	0.79
	B	Quadratic	*0.0283*	*34.53*	ΔT_{peak} (°C) = + 0.08SA% + 0.24LC% − 0.04P80% − 0.01SA%.LC% − 0.005LC%.P80%	0.99
Excipient decomposition	A	Quadratic	*0.0206*	*17.71*	ΔT_{peak} (°C) = − 0.32SA% − 0.007LC% − 0.06TAU% − 0.03SA%.TAU%	0.95
	B	Linear	*0.0451*	*7.42*	ΔT_{peak} (°C) = − 0.35SA% − 0.007LC% − 0.15P80%	0.79
Stability	A	Quadratic	*0.0023*	*427.71*	r = + 0.020SA% + 0.020LC% + 0.009TAU% + 0.0002SA%.TAU% + 0.0004LC%.TAU%	0.99
	B	Quadratic	*0.0399*	*10.97*	r = + 0.02SA% + 0.02LC% + 0.02P80% − 0.0009SA%.P80%	0.92

TAU was the only excipient that did not change the melting peak of TML (Figure 3.2A); however, a significant interaction of this surfactant with LC was observed, resulting in an retardation of TML melting event (negative term in predictive equation of Table 3.2).

According to surface response for TML melting peak variation (Figure 3.2), P80 is the component that has more influence on this response, strongly shifting the melting peak to higher temperatures (darker regions of Figure 2B). In the predictive equation for design B, the coefficient for P80 is much higher than those related to the other two components (Table 3.2). P80 has multiple proton acceptors in its molecular structure that could form hydrogen bond with the proton donor of TML (KUMBHAR; POKHARKAR, 2013). The increase of intermolecular forces hinders drug phase transition, enhancing TML melting peak (WESTWELL et al., 1995).

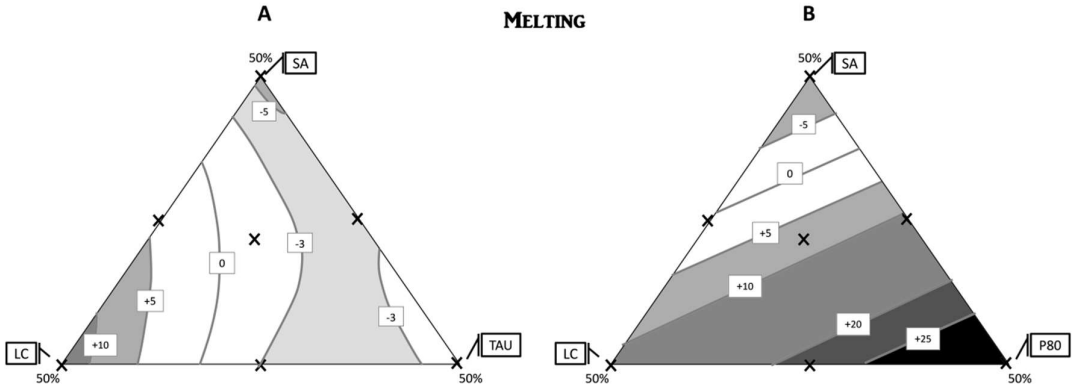

Figure 3.2. Response surface for thymol (TML) melting according to mixture designs A and B. Dark areas show regions with higher thermal interaction. LC: soybean lecithin; P80: polysorbate 80; SA: stearic acid; TAU: sodium taurodeoxycholate.

TML evaporation is a critical property for the preparation of NLC, which requires heating. This can cause loss of the drug at temperatures above 50 °C. In some of the studied systems, the presence of excipients in composition stabilized TML by increasing its evaporation temperature (Figure 3.3). This effect was more pronounced in samples containing LC. The TML+LC mixture, for example, showed an increase in evaporation peak of approximately 12 ºC. The solvation and subsequent solubilization of TML in the phospholipid stabilized the mixture, delaying drug evaporation. However, the opposite effect was observed in some mixtures, as such containing TAU, where an anticipation of the drug evaporation was detected (Figure 3.3).

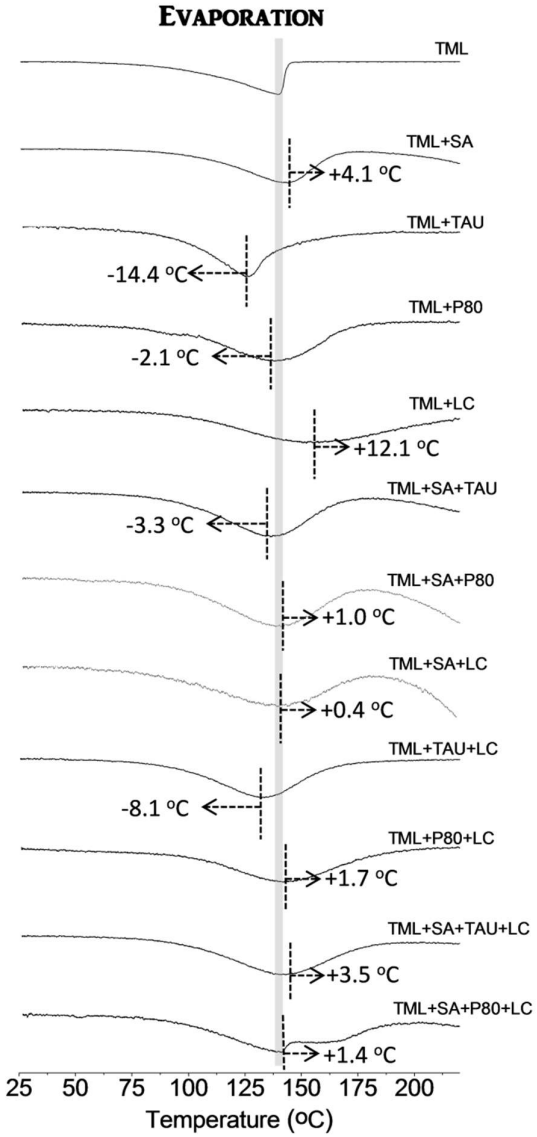

Figure 3.3. First derivative from mass loss TG curves of thymol (TML) and its mixtures according to the mixture designs. T_{peak} for TML evaporation is shaded and the shifts on T_{peak} are indicated in each mixture. LC: soybean lecithin; P80: polysorbate 80; SA: stearic acid; TAU: sodium taurodeoxycholate.

Dark regions in Figure 3.4 indicate compositions with greater TML physical stability, representing more adequate compositions for the preparation of TML-loaded NLC. Predictive equations (Table 3.2) highlight the role of SA and LC in promoting an increase in TML evaporation temperature (positive sign in the equations). The surfactants (TAU and P80), on the other hand, act by reducing the temperature at which this phenomenon occurs (negative sign in the equations). TAU is the most relevant factor for this answer, since its coefficient shows

the highest numerical value in equation (Table 3.2). Also, the negative interaction between SA and LC and, between LC and P80, represents an antagonistic action of these components, reducing TML physical stability (Table 3.2).

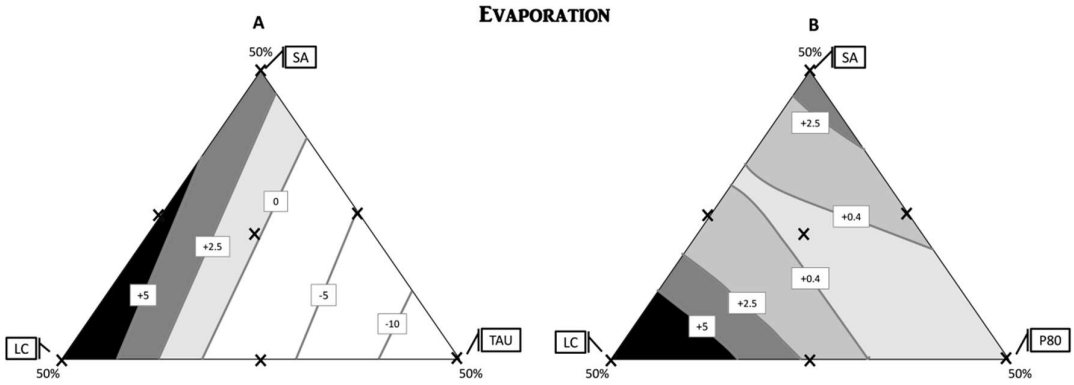

Figure 3.4. Response surface for thymol (TML) evaporation according to mixture designs A and B. Dark areas show regions with TML higher physical stability. LC: soybean lecithin; P80: polysorbate 80; SA: stearic acid; TAU: sodium taurodeoxycholate.

Systems decomposition degree measured by TGA is an important parameter to access sample stability. The use of the first derivative of mass loss curves provided by TGA allows distinguishing the decomposition events of each component, even in complex mixtures (SILVA et al., 2016a). Figure 3.5 shows the T_{peak} related to these events and highlights the shifts on this value comparing to the behavior observed for each isolated material. The shifts were calculated based on the component that first underwent decomposition in the mixture.

Almost all mixtures showed anticipation of excipient decomposition, except for TML+LC sample (Figure 3.5). Complex samples containing three or four components revealed more marked reduction in stability, which reinforces the need to study the compatibility of systems considering the combination of multiples components. Some of those mixtures, e.g. TML+SA+TAU and TML+SA+LC+P80, anticipated the expected decomposition temperature in more than 20°C (Figure 3.5).

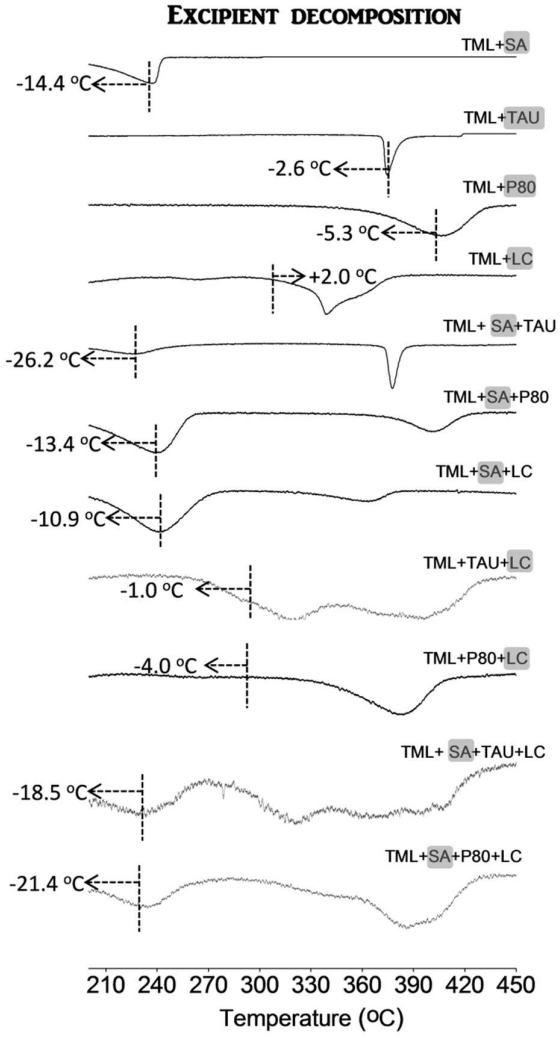

Figure 3.5. First derivative from mass loss TGA curves of thymol (TML) and its mixtures according to the mixture designs. The shifts on T_{peak} for TML excipient decomposition shaded are indicated in each mixture. LC: soybean lecithin; P80: polysorbate 80; SA: stearic acid; TAU: sodium taurodeoxycholate.

In this case, the region of response surface that best preserves the sample involves higher concentrations of LC (Figure 3.6). The inert relation of LC with TML could be related to the solubilization of the drug in this lipid, as previously observed. According to the predictive equation (Table 3.2), LC showed the lowest coefficient value for this answer. The opposite behavior was observed for SA, which had a negative signal and the largest coefficient value, indicating that this component makes the sample less stable at high temperatures (Table 3.2). A negative interaction was observed between SA and TAU, as well as between SA and LC,

which showed the association of these components has an antagonistic effect on system stability (Table 3.2).

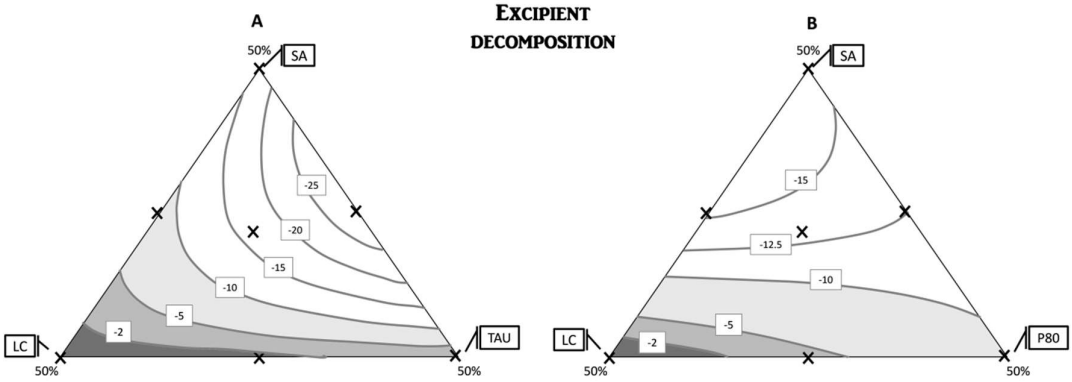

Figure 3.6. Response surface for thymol (TML) excipient decomposition according to mixture designs A and B. Dark areas show regions with excipient higher stability. LC: soybean lecithin; P80: polysorbate 80; SA: stearic acid; TAU: sodium taurodeoxycholate.

3.5.2. Spectroscopic studies

Each formulation isolated compound and in blends was analyzed by FTIR before and after thermal stress. In order to obtain a numerical response representative from FTIR data for the mixture design evaluation, a correlation coefficient (r) was calculated based on the similarity between the spectra before and after thermal stress. Values of $r > 0.9$ indicated a good level of structural similarity between the samples (MECOZZI; PIETROLETTI; MONAKHOVA, 2016). The analysis of individual compounds before and after thermal stress showed r within this limit, indicating the treatment used preserves integrally the spectroscopic profile of the components alone. In the mixtures, the values for r ranged between 0.9992 and 0.8119, suggesting incompatibilities in some samples.

Similarly to thermal analysis results, better stability was achieved with higher proportions of LC (darker areas in Figure 3.7). In turn, TAU exerted a negative effect on the system stability (blank areas in Figure 3.7A), showing the smallest coefficient on predictive equation. In addition, the excipient interacted with the two lipid components (SA and LC) compromising the stability of the sample (Table 3.2). The substitution of TAU by P80 in design B showed that compounds either alone or in certain proportions produce stablw systems; however, a negative interaction between SA and O80 is observed, wich decrease the stability of the sample in higher amounts of those components (Table 3.2, blank area in Figure 3.7B).

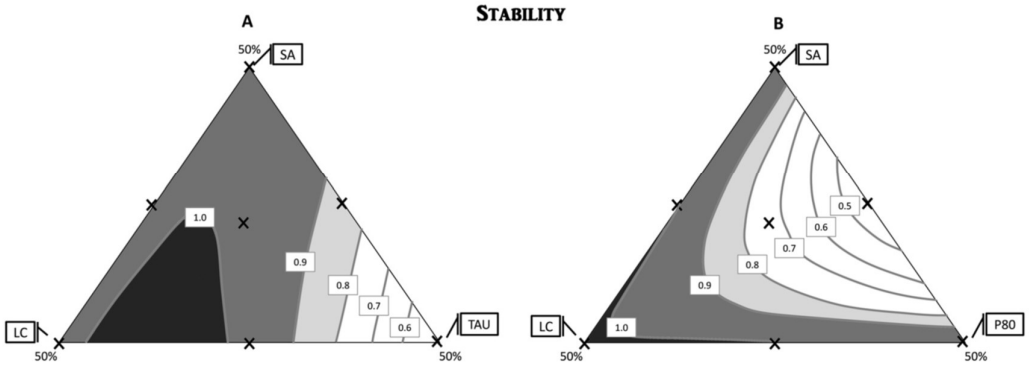

Figure 3.7. Response surface for thymol (TML) excipient decomposition according to mixture designs A and B. Dark areas show regions with higher formulation stability. LC: soybean lecithin; P80: polysorbate 80; SA: stearic acid; TAU: sodium taurodeoxycholate.

In total, three of the analyzed mixture presented r value below the acceptable limit of similarity (Figure 3.8). After thermal stress, the binary mixture of TML and TAU and the ternary mixture of TML, SA and TAU, showed a displacement of the peaks related to the -OH stretch and C-O stretch (at 3360 $cm^{-1}$and 1205 cm^{-1}, respectively). The ternary mixture of TML, SA and P80 also presented some differentiation in peaks relating to the -OH stretch and the C-O stretches (at 3430 cm^{-1} and 1222 cm^{-1}, respectively). Those displacements could be a result of hydrogen bond between the hydroxyl group, which acts as a hydrogen bond donor and the carbonyl group, which acts as a hydrogen bond acceptor (KUMBHAR; POKHARKAR, 2013; LU et al., 2011). However, the sum of the modification in the spectra together with the changes in position and relative intensity of the peaks, especially in the sample TML+SA+TAU, suggests more than a physical interaction, indicating sample decomposition.

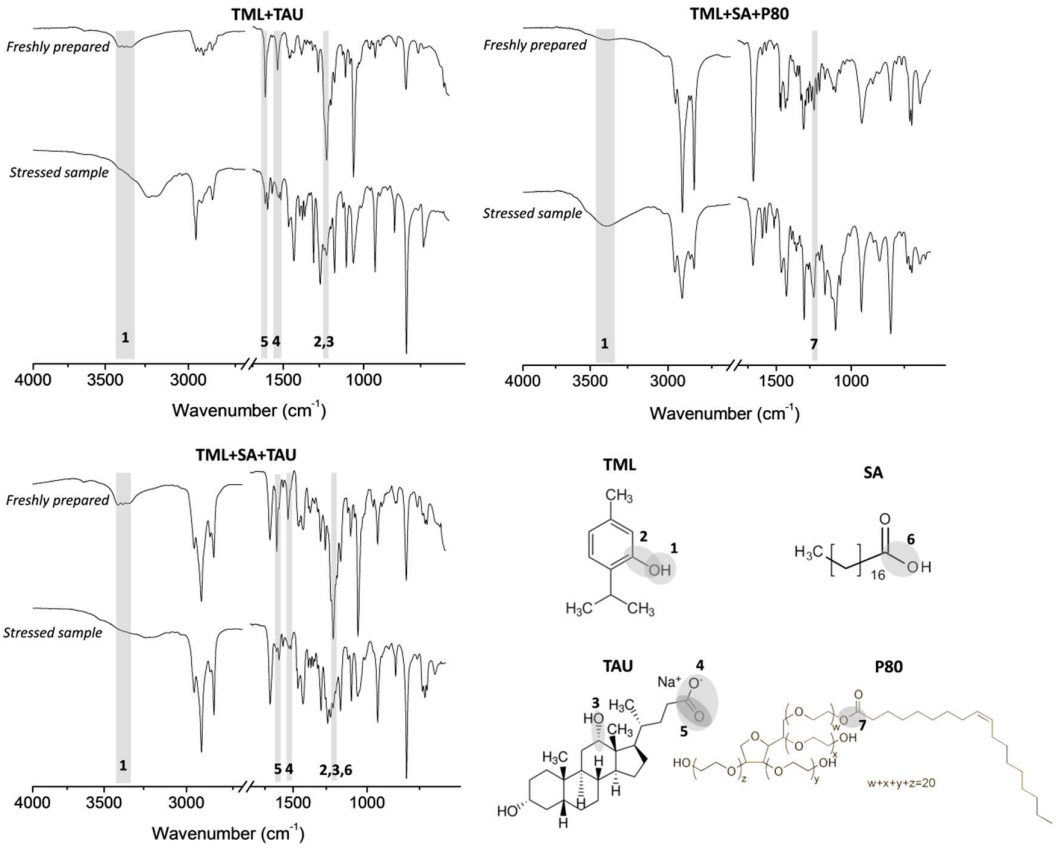

Figure 3.8. Chemical structures of the compounds and FTIR spectra of selected mixtures before and after thermal treatment. Changes in the spectrum are shaded and numbered according to the functional groups involved. LC: soybean lecithin; P80: polysorbate 80; SA: stearic acid; TAU: sodium taurodeoxycholate, TML: thymol.

3.6 CONCLUSION

Even though TAU did not interact with TML when in solid state, after drug melting, physical and chemical instability could be observed, drug evaporation and decomposition were anticipated, and significant changes in infrared spectra were observed. SA, in turn, did not compromise TML stability alone, but demonstrated negative interaction when in combination with other formulation components. LC solubilized TML, elevating the evaporation temperature and benefiting system chemical stability when presented in higher proportions. P80 exerted great influence on TML thermal events; still without compromising physical or chemical stability. This surfactant therefore must be a good alternative to the development of nanostructured lipid systems containing TML.

Although the quantitative delineation of formulation components will be defined by production and performance parameters, the safest formulation to enhance the stability of nanostructured lipid carriers containing TML should comprise P80 as a sulfactant and higher amounts of LEC, while keeping SA concentration in low levels. The use of mixture design in drug-excipient compatibility studies was able to provide more complete information on drug stability profile and guide the development of stable formulations.

3.7 ACKNOWLEDGMENTS

This research was supported by Brazilian agencies CNPq, CAPES and FAP-DF.

3.7 REFERENCES

ALVES-SILVA, I.; SÁ-BARRETO, L. C. L.; LIMA, E. M.; CUNHA-FILHO, M. S. S. Preformulation studies of itraconazole associated with benznidazole and pharmaceutical excipients. **Thermochimica Acta**, v. 575, p. 29–33, 2014.

ANDRADE, L. M.; ROCHA, K. A. D.; DE SÁ, F. A. P.; MARRETO, R. N.; LIMA, E. M.; GRATIERI, T.; TAVEIRA, S. F. Voriconazole-loaded nanostructured lipid carriers for ocular drug delivery. **Cornea**, v. 35, n. 6, p. 866–871, 2016.

BETHANIS, K.; TZAMALIS, P.; TSORTEKI, F.; KOKKINOU, A.; CHRISTOFORIDES, E.; MENTZAFOS, D. Structural study of the inclusion compounds of thymol, carvacrol and eugenol in β-cyclodextrin by X-ray crystallography. **Journal of Inclusion Phenomena and Macrocyclic Chemistry**, v. 77, n. 1–4, p. 163–173, 2013.

CAMPISI, B.; CHICCO, D.; VOJNOVIC, D.; PHAN-TAN-LUU, R. Experimental design for a pharmaceutical formulation: Optimisation and robustness. **Journal of Pharmaceutical and Biomedical Analysis**, v. 18, n. 1–2, p. 57–65, 1998.

CAMPISI, B.; VOJNOVIC, D.; CHICCO, D.; PHAN-TAN-LUU, R. Melt granulation in a high shear mixer: Optimization of mixture and process variables using a combined experimental design. **Chemometrics and Intelligent Laboratory Systems**, v. 48, n. 1, p. 59–70, 1999.

CUNHA-FILHO, M. S. S.; MARTÍNEZ-PACHECO, R.; LANDÍN, M. Compatibility of the antitumoral β-lapachone with different solid dosage forms excipients. **Journal of Pharmaceutical and Biomedical Analysis**, v. 45, n. 4, p. 590–598, 2007.

ERIKSSON, L.; JOHANSSON, E.; WIKSTROM, C. Mixture design — design generation , PLS analysis , and model usage. 1998.

KANG, L.; JUN, H. W.; MANI, N. Preparation and characterization of two-phase melt systems of lidocaine. **International Journal of Pharmaceutics**, v. 222, n. 1, p. 35–44, 2001.

KUMBHAR, D. D.; POKHARKAR, V. B. Colloids and Surfaces A : Physicochemical and Engineering Aspects Engineering of a nanostructured lipid carrier for the poorly water-soluble drug , bicalutamide : Physicochemical investigations. **Colloids and Surfaces A: Physicochemical and Engineering Aspects**, v. 416, p. 32–42, 2013.

LEE, S.-J.; UMANO, K.; SHIBAMOTO, T.; LEE, K.-G. Identification of volatile components in basil (Ocimum basilicum L.) and thyme leaves (Thymus vulgaris L.) and their antioxidant properties. **Food Chemistry**, v. 91, p. 131–137, 2005.

LU, P.; ZHANG, M.; LIU, Y.; LI, J.; XIN, M. Characteristics of Vermiculite-Reinforced Thermoplastic Starch Composition Films. **Journal of Applied Polymer Science**, p. E117–E122, 2011.

MARCHESE, A.; ORHAN, I. E.; DAGLIA, M.; BARBIERI, R.; LORENZO, A. DI; NABAVI, S. F.; GORTZI, O.; IZADI, M.; NABAVI, S. M. Antibacterial and antifungal activities of thymol: a brief review of the literature. **Food Chemistry**, v. 210, p. 402–414, 2016.

MAXIMIANO, F. P.; NOVACK, K. M.; BAHIA, M. T.; DE SÁ-BARRETO, L. L.; DA CUNHA-FILHO, M. S. S. Polymorphic screen and drug-excipient compatibility studies of the antichagasic benznidazole. **Journal of Thermal Analysis and Calorimetry**, v. 106, n. 3, p. 819–824, 2011.

MECOZZI, M.; PIETROLETTI, M.; MONAKHOVA, Y. B. FTIR spectroscopy supported by statistical techniques for the structural characterization of plastic debris in the marine environment: Application to monitoring studies. **Mpb**, v. 106, p. 155–161, 2016.

MURA, P.; FURLANETTO, S.; CIRRI, M.; MAESTRELLI, F.; MARRAS, A. M.; PINZAUTI, S. Optimization of glibenclamide tablet composition through the combined use of differential scanning calorimetry and D-optimal mixture experimental design. **Journal of Pharmaceutical and Biomedical Analysis**, v. 37, n. 1, p. 65–71, 2005.

MURA, P.; GRATTERI, P.; FAUCCI, M. T. Compatibility studies of multicomponent tablet formulations: DSC and experimental mixture design. **Journal of Thermal Analysis and Calorimetry**, v. 68, n. 2, p. 541–551, 2002.

PROW, T. W.; GRICE, J. E.; LIN, L. L.; FAYE, R.; BUTLER, M.; BECKER, W.; WURM, E. M. T.; YOONG, C.; ROBERTSON, T. A.; SOYER, H. P.; ROBERTS, M. S. Nanoparticles and microparticles for skin drug delivery. **Advanced Drug Delivery Reviews**, v. 63, n. 6, p. 470–491, 2011.

RIELLA, K. R.; MARINHO, R. R.; SANTOS, J. S.; PEREIRA-FILHO, R. N.; CARDOSO, J. C.; ALBUQUERQUE-JUNIOR, R. L. C.; THOMAZZI, S. M. Anti-inflammatory and cicatrizing activities of thymol, a monoterpene of the essential oil from Lippia gracilis, in rodents. **Journal of Ethnopharmacology**, v. 143, n. 2, p. 656–663, 2012.

SHAH, S. M.; JAIN, A. S.; KAUSHIK, R.; NAGARSENKER, M. S.; NERURKAR, M. J. Preclinical Formulations: Insight, Strategies, and Practical Considerations. **AAPS PharmSciTech**, v. 15, n. 5, p. 1307–1323, 2014.

SHAHIDI, F.; ZHONG, Y. Lipid oxidation and improving the oxidative stability. **Chemical Society reviews**, v. 39, n. 11, p. 4067–79, 2010.

SILVA, L. A. D.; ANDRADE, L. M.; DE SÁ, F. A. P.; MARRETO, R. N.; LIMA, E. M.; GRATIERI, T.; TAVEIRA, S. F. Clobetasol-loaded nanostructured lipid carriers for epidermal targeting. **Journal of Pharmacy and Pharmacology**, v. 68, n. 6, p. 742–750, 2016a.

SILVA, L. A. D.; TEIXEIRA, F. V.; SERPA, R. C.; ESTEVES, N. L.; DOS SANTOS, R. R.; LIMA, E. M.; DA CUNHA-FILHO, M. S. S.; DE SOUZA ARAÚJO, A. A.; TAVEIRA, S. F.; MARRETO, R. N. Evaluation of carvedilol compatibility with lipid excipients for the development of lipid-based drug delivery systems. **Journal of Thermal Analysis and Calorimetry**, v. 123, n. 3, p. 2337–2344, 2016b.

TASDEMIR, D.; KAISER, M.; DEMIRCI, F.; BASER, K. Essential oil of Turkish Origanum onites L. and its main components, carvacrol and thymol show potent antiprotozoal activity without cytotoxicity. **Planta Med**, v. 72, n. October 2016, p. 1006, 2006.

WECHSLER, J. B.; HSU, C. L.; BRYCE, P. J. IgE-mediated mast cell responses are inhibited

by thymol-mediated, activation-induced cell death in skin inflammation. **Journal of Allergy and Clinical Immunology**, v. 133, n. 6, p. 1735–1743, 2014.

WESTWELL, M. S.; SEARLE, M. S.; WALES, D. J.; WILLIAMS, D. H. Empirical Correlation between Thermodynamic Properties and Intermolecular Forces. **Journal of the American Chemical Society**, v. 117, n. 18, p. 5013–5015, 1995.

WU, L.; ZHANG, J.; WATANABE, W. Physical and chemical stability of drug nanoparticles. **Advanced Drug Delivery Reviews**, v. 63, n. 6, p. 456–469, 2011.

ZHANG, N.; YUAN, Y.; DU, Y.; CAO, X.; YUAN, Y. Preparation and properties of palmitic-stearic acid eutectic mixture/expanded graphite composite as phase change material for energy storage. **Energy**, v. 78, p. 950–956, 2014.

CHAPTER 4- NANOSTRUCTURED LIPID CARRIERS LOADING THYMOL OR *Lippia origanoides* ESSENTIAL OIL COMPLEXED WITH CYCLODEXTRIN FOR DERMATOLOGICAL APPLICATION

The aim of this part of the work was to obtain the most efficient and stable solid inclusion complexes of TML and essential oil of *Lippia origanoides* (EO) from a screening of different CDs types and methodologies further inserted in NLC systems. The effect of complexation in drug physicochemical properties were assessed together with its influence on drug skin permeation.

4.3 MATERIAL AND METHODS

4.3.1 Materials

TML (Lot SZBF0370V, purity ≥ 99%) was purchased from Sigma-Aldrich (Steinheim, Germany). *Lippia origanoide* essential oil (EO) containing 88.2% of TML was extracted from the aerial parts of the plant by hydrodistillation, the extraction was made in the Federal University of Pará, on the laboratory of natural products engineering. The α-cyclodextrin (αCD**),** β-cyclodextrin (βCD)**,** γ-cyclodextrin (γCD) and hydroxypropyl-β-cyclodextrin (HPβCD) were donated by Ashland Specialty Ingredients (Covington, LA, USA). Stearic acid, soybean lecithin and polysorbate 80 were purchased from Sigma-Aldrich (Steinheim, Germany), Lipoid (Ludwigshafen, Germany), and Merck (Darmstadt, Germany), respectively. Sodium dodecyl sulfate purchased from Dinamica Química Contemporânea Ltda (São Paulo, Brazil), used to prepare solutions applied in multiple assays. Cellulose acetate membrane (MW 12,000-14,000) were purchased from Fisher (Pittsburg, KS, USA). Scotch Book Tape N0. 845 (3M, St Paul, MN, USA) was used for tape stripping and cyanoacrylate superglue (Henkel Loctite, Dublin, Ireland) was used for follicle biopsies. The solvents used during the study were all of HPLC grade purchased from Tedia (Rio de Janeiro, Brazil). The water used in all preparations was of Milli-Q grade (Millipore, Illkirch-Graffenstaden, France).

Porcine ear skin was used in permeation assay. The ears were obtained from local abattoir (Bonasa Alimentos, São Sebastião, Brazil) less than 2h after the animal´s sacrifice. The whole skin was romoved from the outer region of the ear, separated from it´s underlying layers and used “full-tickness”. The skin was stored frozen at -20 °C for a maximum of 1 month before use.

4.3.2 Drug assay

For the permeation studies, a reversed-phase high performance liquid chromatography (HPLC) method was used selective against skin interferents (ANGELO et al., 2016). The analyses were carried out on a LC-20AD instrument (Shimadzu, Kyoto, Japan) with injection volume of 30 µL using a column RP-C18 (300 mm x 3.9 mm; 10 µm) settled at 40 °C. The mobile phase was acetonitrile and water 35:65 v:v with a flow rate of 1.5 mL min^{-1} and detection at 278 nm. For TML determination in inclusion complexes, NLC formulations, and for dissolution and drug release studies some adjustments were performed (flow rate of 1.2 mL min^{-1} and acetonitrile/water 50:50 v:v as mobile phase). This method was validated following the International Conference on Harmonization parameters. Selectivity against all possible interferents was performed without statistical interferences in drug determination. The linearity showed a correlation coefficient (r) of 0.998 with the slope different of zero and the residues randomly distributed without tendency.

4.3.4 Phase solubility diagrams

Phase solubility diagrams were built based on Higuchi and Connors methodology (HIGUCHI; CONNOR, 1965). An excess amount of TML was added to an aqueous solution containing CDs in increasing concentrations (0 to 5% w/v) and placed to sealed ampoules. The suspensions were agitated in an orbital shaker KJ-201BD (IKA®, Staufen, German) for 72h at room temperature. Then, they were filtered (0.45 µm) and TML concentration were obtained by the previous described HPLC method. αCD, βCD, γCD and HPβCD samples were assayed for TML content. The experiments were conducted in triplicate.

The stability constant of the complexes ($K_{1:1}$) was calculated from the linear regression of experimental data, according to Eq. 1:

$$K_{1:1} = \frac{\text{Slope}}{\text{So}(1-\text{Slope})} \qquad \text{(Eq. 1)}$$

where So was the intrinsic solubility of TML in water.

In addition, complexation efficiency (CE) was calculated according to the Eq. 2 (LOFTSSON; HREINSDÓTTIR; MÁSSON, 2005)

$$\text{CE} = \text{So}K_{1:1} = \frac{[D/CD]}{[CD]} = \frac{Slope}{1-Slope} \qquad \text{(Eq. 2)}$$

where the *[D/CD]* was the concentration of dissolved complex; and *[CD]* was the concentration of free CD.

4.3.5 Preparation of the solid inclusion complexes

The mixtures of TML or EO with HPβCD in an equimolar ratio were submitted to different technologies to produce solid inclusion complexes as following.

4.3.5.1 Freeze drying (FD)

A molar equivalent of TML or EO were added to an 20% solution of HPβCD in ethanol 10%, under magnetic stirring (1200 rpm). The solution was agitated on an orbital shaker for 72 h. After this time, the mixture was frozen at -80 °C and then lyophilized in a AdVantage Plus XL-70 freeze dryer (SP Scientific, Warminster, USA) for 48 h.

4.3.5.2 Spray drying (SD)

A molar equivalent of TML or EO were added to an 20% solution of HPβCD in ethanol 10%, under magnetic stirring (1200 rpm). The solution was agitated on an orbital shaker for 72 h. The mixture was atomized by a spray dryer MSD 1.0 (Labmaq, Ribeirão Preto, Brazil) with a 1.0 mm pressurized atomizer using a feed rate of 2.3 mL min^{-1}, with an inlet temperature of 125 °C and an atomizing airflow rate of 3.9 m^3 min^{-1}.

4.3.5.3 Rotary-evaporation (RE)

A molar equivalent of TML or EO were added to an 20% solution of HPβCD in ethanol, under magnetic stirring (1200 rpm). The solution was agitated on an orbital shaker for 72 h and then transferred to a round balloon flask. The solvent was evaporated by a rotary evaporator model Rotavapor® R300 (Buchi, Flawil, Switzerland) maintained in a temperature of approximately 80 °C and in constant rotation.

4.3.5.4 Supercritical CO_2 ($SCCO_2$)

Samples were processed in a supercritical laboratory scale unit, comprised by a CO_2 cylinder (Air Liquide Brasil Ltda., 95% purity), two syringe pumps (Teledyne Isco, Model 500D), two thermostatic baths (Quimis, Model Q214M2 and Tecnal, ModelTE-184), and one cell with internal volume of approximately 170 mL (base diameter 2.85 cm and height 26.1

cm). The materials were maintained static and samples were processed under pressure of 250 bar and temperature of 50 °C using two different time processing: 3 and 6 h.

4.3.6 Characterization of the inclusion complexes

4.3.6.1 Scanning electron microscopy (SEM)

A minimaum amount of the samples were previously coated with gold and analyzed using a Quanta 250 FEG equipment (FEI, Oregon, USA).

4.3.6.2 Fourier transform infrared spectroscopy (FTIR)

The FTIR analyses were performed using a Varian 640-IR FTIR spectrometer (Agilent Technologies, Santa Clara, USA). The spectra of the samples were recorded between 400 cm^{-1} and 4000 cm^{-1} using an ATR imaging accessory. Some of the resulting spectra were analyzed considering the correlation coefficient (r) between the samples, calculated by the Essential FTIR software (Operant LLC).

4.3.6.2 Thermal analysis

Differential scanning calorimetry (DSC) and thermogravimetric (TG) analyses were performed in a DSC-60 and DTG-60, respectively (Shimadzu®, Tokyo, Japan), under nitrogen controlled atmosphere with flow of 50 mL min^{-1}. Samples of approximately 3 mg were analyzed under a heating rate of 5 $^{o}C\ min^{-1}$ from 25 to 500 ^{o}C. All thermal measurements were performed using the TA-60 Shimadzu® software.

4.3.6.2 Dissolution rate

The dissolution profiles were determined in a dissolution tester Ethik model 299 (Nova Ética, São Paulo, Brazil) using water as a medium. Temperature was maintained at 25 °C and paddle speed was adjusted to 100 rpm. Samples containing an equivalent amount of 2 mg of TML were added to the dissolution vessel. Aliquots were withdrawn at predetermined times, filtered (0.45 μm) and properly quantified using the chromatographic method described before. Experiments were performed in triplicate and dissolution profiles were evaluated using its correspondent dissolution efficiency at 30 min (DE_{30}) (SÁ-BARRETO et al., 2013).

4.3.7 Production of nanostructured lipid carriers (NLCs)

NLCs were produced using the method of microemulsion dilution. A microemulsion was prepared using as the external phase water and as internal phase an oily mixture of stearic acid (15 mg/mL) and oleic acid (5 mg/mL). The surfactants used were soy lecithin (10 mg/mL) and polysorbate 80 (2.5 mg/mL). Previous preformulation studies proved the compatibility between the compounds selected for NLC preparation (PIRES et al., 2017).

Internal phase compounds were mixture with the surfactants and heated at 80 °C until the complete melting of the lipids. After that, TML or EO as supplied or in their solid inclusion complexes form were added (equivalent to 800 µg/mL of TML) and maintaining under stirring (800 rpm) for 10 min. The next step was the addition of a water (also heated at 80 °C) under stirring in order to form a microemulsion. Then, the heated microemulsion was dripped into a 0.2 M buffer phosphate solution pH 5.4 maintained on ice bath under intense stirring using an ultra-turrax® (IKA-Werk GmbH&Co. KG, Staufen, Germany) at 15000 rpm during 20 min. The proportion microemulsion:buffer solution used was 1:20 (v/v) (SILVA et al., 2016).

4.3.8 Characterization of the NLCs

4.3.8.1 Particle size, polydispersity index and zeta potential

Particle size, polydispersity index (PDI) were determined by dynamic light scattering and zeta potential by electrophoretic mobility, after the dilution of NLC dispersions in water, using a Zetasizer Nanoseries (Malvern Instruments, Worcestershire, UK). Each measure was performed in triplicate at 25 °C.

4.3.8.2 Entrapment efficiency and drug loading

Drug entrapment efficiency (EE) and drug loading (DL) were calculated using equations 3 and 4, respectively.

$$\mathrm{EE\%} = \frac{(TD-FF)}{TD} \times 100 \qquad \text{(Eq. 3)}$$

$$\mathrm{DL\%} = \frac{(TD-FF)}{TL} \times 100 \qquad \text{(Eq. 4)}$$

The total amount of TML (TD) in each NLC dispersion was determined by HPLC after proper dilution in methanol. NLC dispersion were centrifuged in a concentrator Vivaspin 2

MWCO 10,000 (Vivascience AG, Hannouver, Germany) for 10 min at 2700g on a centrifuge Z 306 (Hermle Labortechnik GmbH, Wehingen, Germany) and the amount of the drug not entrapped (NE) was obtained by quantifying the TML in the liquid filtered by the concentrator, named filtered fraction (FF).

where TD is the concentration of the TML in the suspensions before centrifugation, FF is the concentration of the TML not entrapped, and TL is the total amount of the lipids on the formulation.

4.3.8.3 pH

The pH of the NLCs dispersions were determined using a Digimed DM-22 pHmeter (Digimed Analytica Ltda., São Paulo, Brazil). Standard buffer solutions (pH 4.0 and 7.0) were used to calibrate the instrument before use.

4.3.8.4 Drug release studies

The *in vitro* release profile of TML from the different formulations was determined using samples containing the equivalent of 800 μg mL^{-1} of TML in modified Franz-type diffusion cell thermostated at 35 °C containing in the donor chamber the sample, and in the receptor chamber a phosphate buffer solution pH 7.0 for the TML samples, and a 0.5% (w/v) sodium dodecyl sulfate solution for the EO samples. The two chambers were separated by a hydrophilic cellulose membrane. The kinetic was followed during 24h.

4.3.8.5 Drug permeation studies

The modified Franz-type diffusion cell was assembled with the skin of the porcine ear separating the donor to the receptor chambers. The receptor chamber was filled with 0.2 mol L^{-1} phosphate buffer pH 7.0 for TML samples, and 0.5% (w/v) sodium dodecyl sulfate solution for EO samples. In the donor chamber, it was added the NLC formulations and control solutions both with TML concentration of 800 μg mL^{-1}.

At end of each series of experiment the receptor solution was withdrawn from the diffusion cell and analyzed by for TML content in HPLC. The skin was removed from the diffusion cell and placed onto a flat surface, with the stratum corneum (SC) facing up. Was cleaned with ultrapure water, dried with gauze pad and tape-stripped 10 times, using Scotch

Book tapes. After the procedure all the tapes were placed in a recipient with 15 mL of methanol, intense magnetic stirring (1000 rpm) was maintained for 6h, extracting TML from the SC. In the next step a drop of cyanoacrylate superglue was applied to the stripped skin area and a tape was placed above the glue, after drying the tape were stripped in one movement, extracting the hair follicles (HF) of the skin. The process is repeated for three times and the TML were extracted from the tapes the same way as the SC. The last step was to cut the remaining skin (RS) in small pieces and extract TML of this portion as well. After the extraction process the solvent were withdrawn from the recipients, filtered and analyzed by HPLC.

4.3.9 Statistical analysis

Significance level (p) was fixed at 0.05 and data normality were previously tested. Results were analyzed using one-way ANOVA followed by Turkey post-test for data that showed parametric behavior, and for non-parametric data results were analyzed using Kruskal-Wallis test with Dunn's post-test.

4.4 RESULTS AND DISCUSSION

4.4.1 Cyclodextrin selection

The first step of the study was to select the CD variety to be used in the production of TML solid inclusion complexes. For this, the natural CDs (αCD, βCD and γCD) and the modified HPβCD were tested with TML using phase-solubility diagrams (Table 4.1). All CDs could improve the drug solubility, showing an A_L type phase-solubility diagram with slope less than a unity, which indicates a most likely molar inclusion complex stoichiometry of 1:1 (KURKOV, LOFTSSON, 2013).

Different values of $K_{1:1}$ were found according to the CD type following the order γCD < αCD < βCD < HPβCD (Table 4.1). The stability constant indicates the strength of the complex and its results showed that βCD and its derivative HPβCD, both composed by seven unities of glucose, were more effective in encapsulate the TML, which is in agreement with previous reports (TAO et al., 2014; KFOURY et al., 2016**).** Indeed, molecules with aromatic structures can be better accommodated in the intermediate cavity size of βCD. Furthermore, the presence of the hydroxypropyl groups extends the hydrophobic region of the βCD cavity which can enhance the stability of the complex (CUNHA-FILHO; MARTÍNEZ-PACHECO; LANDIN, 2013).

Table 4.1 Phase solubility diagrams data including thymol intrinsic solubility (*So*); stability constant of the complexes ($K_{1:1}$); correlation constant of the solubility diagram (R^2); slope of the solubility diagram; intercept of the solubility diagram; and complexation efficiency (*CE*).

Cyclodextrin	*So* (10^{-6} *M*)	$K_{1:1}$ (M^{-1})	R^2	*Slope*	*Intercept* (10^{-6} *M*)	*CE*
αCD	5.65	23,803	0.9831	0.1187	6.14	0.135
βCD		73,879	0.6693	0.2948	6.97	0.410
γCD		9,341	0.9263	0.0502	5.41	0.053
HPβCD		125,063	0.9927	0.4144	6.72	0.708

Difference between the experimental intrinsic solubility of TML (So) and the intercept of the phase-solubility diagram could lead to complexation constant not reliable (LOFTSSON; HREINSDÓTTIR; MÁSSON, 2005). Indeed, for some CDs tested, this difference reached more than 20% (Table 1). In order to avoid possible errors, CE, which is independent constant from both values was calculated. Accordingly, the highest values of CE were found for HPβCD (0.708), 1.7 times superior that for βCD and almost 14 times and 5 times greater than CE values found for γCD and αCD, respectively (Table 1). Based on this, HPβCD was selected to produce TML and EO inclusion complexes in solid state.

4.4.2 Preparation and analysis of the solid inclusion complexes

There is not a universal method to produce solid state inclusion complexes with CDs and the choice of an appropriate methodology is usually empirical (MURA, 2015). In this study different methods to produce solid inclusion complexes were tested, namely FD, SD, RE, $SCCO_2$/3h and $SCCO_2$/6h using an equimolar ratio of TML or EO and HPβCD.

For most of the systems, satisfactory results of drug content were obtained (above 90%). However, for TML-SD, EO-SD and EO-$SCCO_2$/3h, the drug content results were 59.1%, 34.2% and 72.5%, respectively. In the case of SD, the high temperatures used to dry the samples (above 100 ºC) possibly have caused the TML evaporation before its encapsulation. Similarly, the unsatisfactory results of EO-$SCCO_2$/3h might have been caused by the evaporation of TML during the depressurization step due to the reduced processing time of the sample. Indeed, the drug content of EO-$SCCO_2$/6h close to 100% reinforces this hypothesis.

All samples seems to present an amorphous appearance according to SEM photomicrographs (Figure 4.1); however certain distinctions between them were denoted. $SCCO_2$ samples showed a similar aspect to PM, which suggests a lower degree of interaction between the components, contrasting to FD and RE samples, which exhibited a more compact and uniform appearance, completely different from PM.

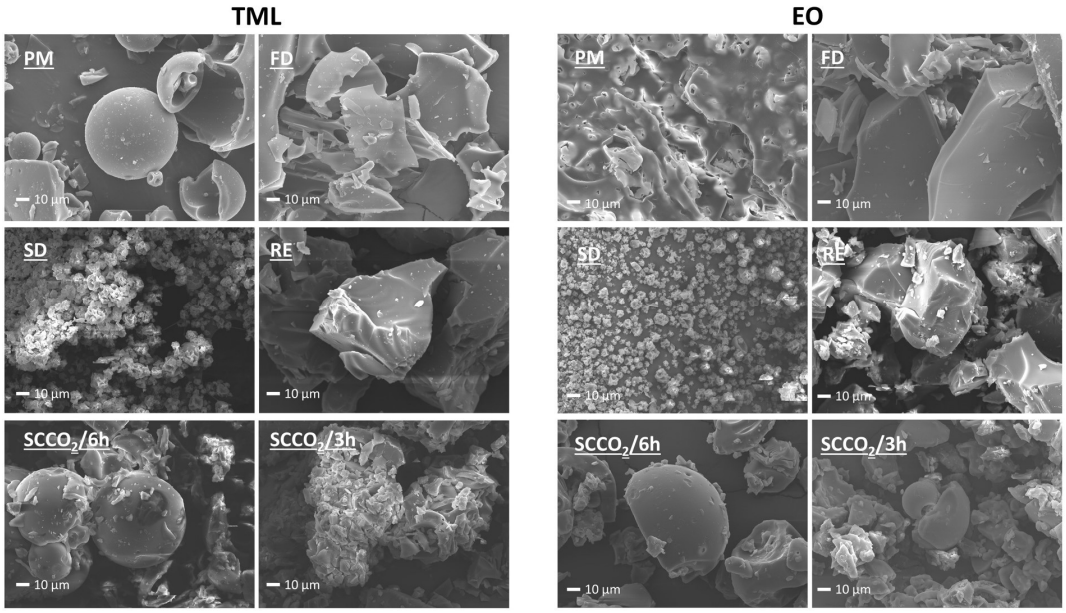

Figure 4.1 SEM photomicrographs of the physical mixture (PM) and the inclusion complexes of thymol (TML) and *Lippia origanoides* essential oil (EO) produced by different methodologies. FD: Freeze Drying; SD: Spray Drying; RE: Rotary-evaporation; $SCCO_2$: Supercritic CO_2.

FTIR analysis was used to investigate the inclusion complex formation based on shifts or intensity changes in the characteristic bands of TML and HPβCD, which could be considered as evidence of the complex existence (MURA, 2015).

The similarity FTIR index values were above 0.98, which confirms the chemical preservation of the sample, corroborating HPLC analyses (PIRES et al., 2017). Nevertheless, a detailed examination of the peaks corresponding to functional groups of both TML and HPβCD revealed changes that may indicate the establishment of intermolecular interactions among the compounds.

Figure 4.2 shows an assembly of selected FTIR analyses, displayed as a representative sample, since no appreciable differences were observed between the complexation methods tested. PM analysis of both TML and EO with HPβCD exhibited an overlap of each spectrum

allowing to identify some characteristics bands of these compounds. For instance, O-H, C_{sp3}-H and C-O stretches appeared at 3,200 cm^{-1}, 2,956 cm^{-1}, and 1,026 cm^{-1}, respectively, for TML; and at 3,342 cm^{-1}, 2,960 cm^{-1}, and 1,031 cm^{-1}, respectively, for EO. The same groups are also presented in HPβCD overlapped. Moreover, C_{sp2}-H and at 804 cm^{-1} for TML and 808 cm^{-1} for EO appeared isolated from HPβCD signals.

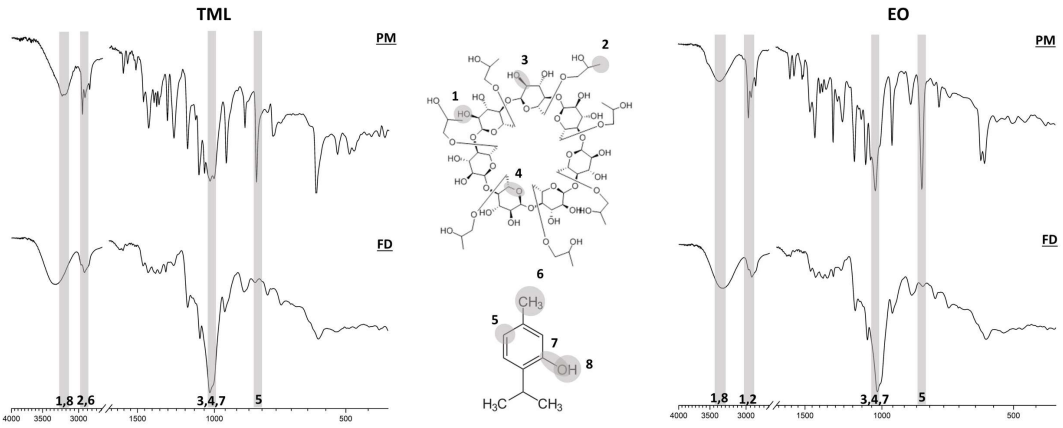

Figure 4.2 FTIR spectra of physical mixture (PM) and the inclusion complexes of thymol (TML) and *Lippia origanoides* essential oil (EO) produced by freeze drying (FD). Changes in the spectrum are shaded and numbered according to the functional groups involved and correlated to its chemical structures.

Small variations on the position of the band correspondent to the groups O-H, C_{sp3}-H and C-O stretches of processed samples occurred as shown on Table 4.2. Some changes are commonly very subtle in inclusion complexes, requiring careful interpretation of the spectra (CUNHA-FILHO et al., 2007). Indeed, O-H and C-O stretches are, respectively, a donor and a receiver of hydrogen bonds, and C_{sp3}-H is responsible for weak interactions between drug-CD evidenced by small shifts at their position in FTIR bands.

In contrast, TML C_{sp2}-H band at 804-808 cm^{-1} was just barely visible in processed samples (Figure 4.2). Probably, a "shield effect" occurred, in which the insertion of TML into the HPβCD cavity inhibited the visualization of this band on the FTIR spectrum (ADEOYE, CABRAL-MARQUES, 2017). Thus, consistent spectroscopic evidences of inclusion complexes formation in samples processed by different methodologies were observed, although a clear distinction among the methods cannot be drawn.

Table 4.2 Selected wavelength of functional groups of physical mixture (PM) and the inclusion complexes of thymol (TML) and *Lippia origanoides* essential oil (EO) produced by different methods. FD: Freeze Drying; SD: Spray Drying; RE: Rotary-evaporation; $SCCO_2$: Supercritic CO_2.

TML							
Functional Group	*Wavelength (λ, cm^{-1})*						**Average Δ λ**
	PM	*Inclusion Complexes*					
		FD	*SD*	*RE*	*$SCCO_2$ 6h*	*$SCCO_2$ 3h*	
v(O-H)	3200	3306	3313	3309	3319	3306	*+110.6*
v(C_{sp3}-H)	2956	2924	2923	2924	2924	2924	*-32.2*
v(C-O)	1026	1024	1028	1026	1028	1024	*0*
v(C_{sp2}-H)oop	804	806	802	806	808	806	*-1.6*
EO							
Functional Group	*Wavelength (λ, cm^{-1})*						**Average Δ λ**
	PM	*Inclusion Complexes*					
		FD	*SD*	*RE*	*$SCCO_2$ 6h*	*$SCCO_2$ 3h*	
v(O-H)	3342	3306	3330	3327	3311	3304	-26.4
v(C_{sp3}-H)	2960	2924	2923	2924	2924	2924	-36.2
v(C-O)	1031	1024	1026	1026	1024	1026	-5.8
v(C_{sp2}-H)oop	808	806	802	808	806	806	-2.4

In the DSC analysis of TML as supplied (Figure 4.3), two endothermic events were observed. The first event was a sharp peak with T_{peak} at 49.4 °C, corresponding to its melting, and the second was a broad peak in the range of 50-120°C, corresponding to its evaporation. DSC of EO is composed by one first event in the same range of TML evaporation, which is the principal component of EO, followed by undistinguished endothermal events. HPβCD, as expected, showed a broad endothermic peak from 30 to 120°C due dehydration and a decomposition starting from 320.0 °C.

DSC profile of PM reveled an overlap of each compound events. Actually, subtle changes occurred on T_{peak} of TML melting (from 49.4 °C to 43.8 °C), probably due an interference of the simultaneous HPβCD dehydration in the same range of temperature.

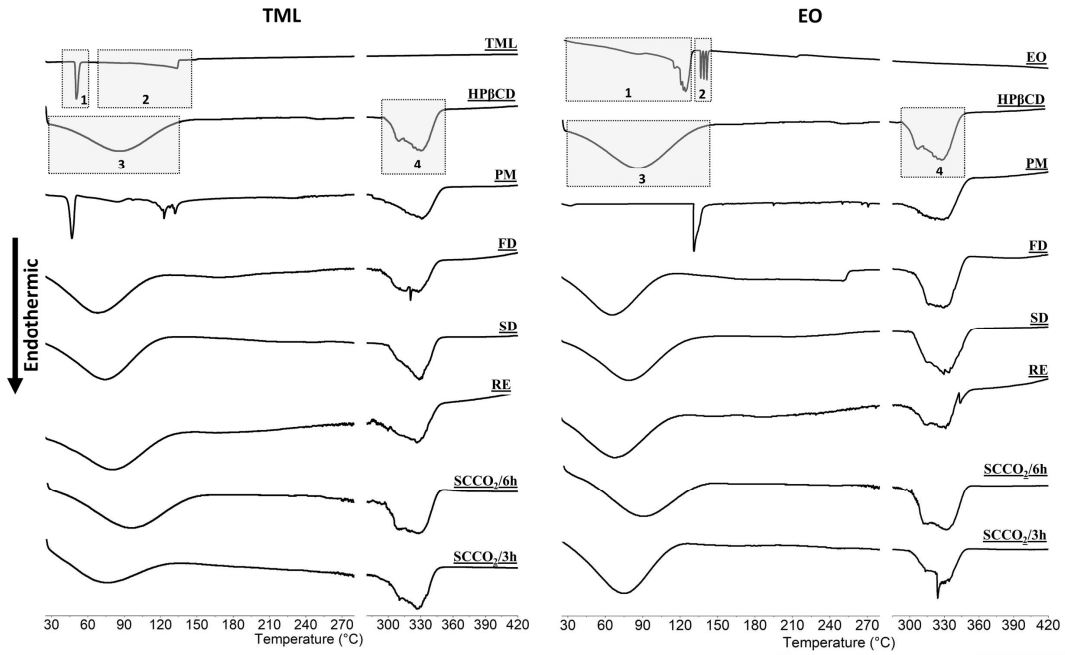

Figure 4.3 DSC analyses of thymol (TML), hydroxypropyl-β-cyclodextrin (HPβCD**)** and *Lippia origanoides* essential oil (EO) as supplied, physical mixtures (PMs) and the inclusion complexes of TML or EO obtained by the different methodologies. Highlighted areas 1-4 represent the main thermal events of the pure materials. FD: Freeze Drying; SD: Spray Drying; RE: Rotary-evaporation; $SCCO_2$: Supercritic CO_2.

DSC of all processed samples exhibited a similar profile without any thermic events that characterizes TML or EO (Figure 4.3). The peaks corresponding to the melting and evaporation of TML or to evaporation of EO were not observed and the samples presented practically the same behavior of the HPβCD as supplied, which is according to other studies involving drug inclusion complex with CD and provide additional proofs of complexation (MURA, 2015).

TG analyses, represented in Figure 4.4 by the first derivative of TG (DrTG), are in agreement with DSC results and, in addition, provide information about encapsulation level in each sample. A single mass loss step (99.9%) was observed in TML as supplied as a result of its evaporation in the range of 40-180 °C (MARRETO et al., 2008). Similarly, EO as supplied showed a mass loss of 98.7% in the same temperature range. HPβCD, as expected, presented an initial mass loss of around 4% in the range of 40-120°C corresponding to dehydration and a second event after 280 °C related to its decomposition with around of 88% of mass loss.

The PMs containing TML or EO showed an initial mass loss of around 10%, corresponding to the dehydration of HPβCD together with the evaporation of almost the entire TML of the sample, which, in theory, represent 10% of the mixture (Figure 4.4). A small mass

loss in the range of 120-280°C is denoted, possibly corresponding to a small fraction of TML that have been encapsulated during the analysis (around 1%). Indeed, *in situ* formation of inclusion complex during thermal analyses have been frequently reported (CUNHA-FILHO et al., 2007; MAXIMIANO et al., 2011).

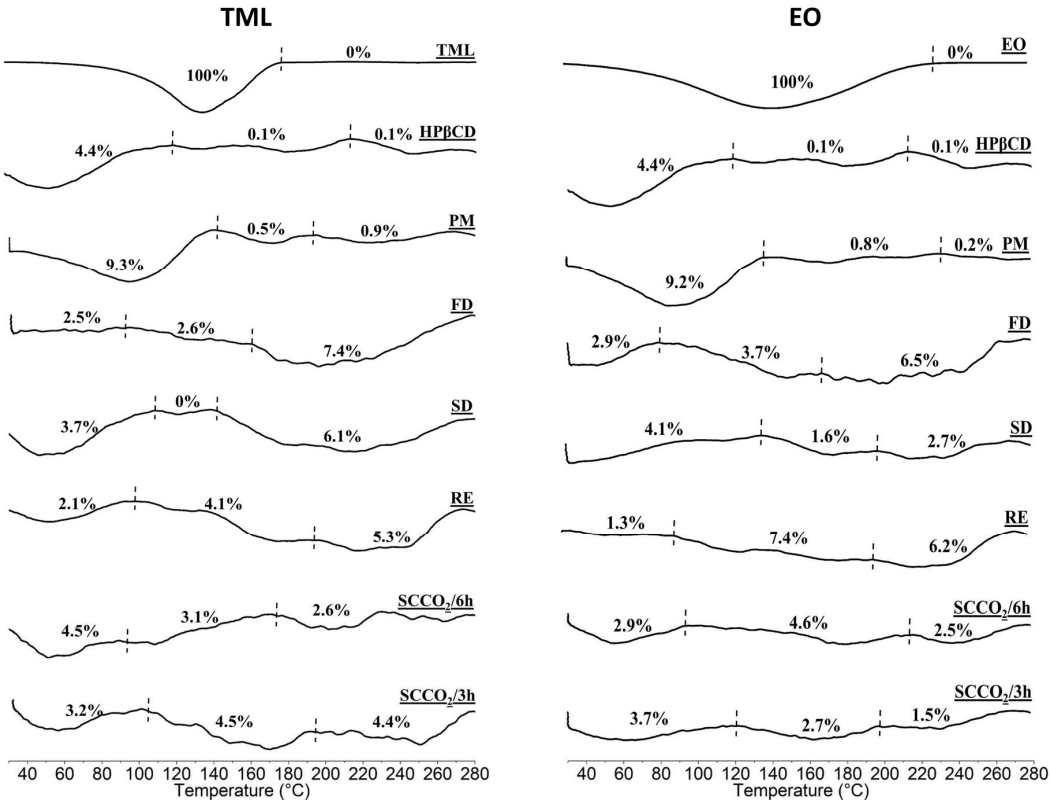

Figure 4.4 First derivative of thermogravimetric analyses (DrTG) of thymol (TML), hydroxypropyl-β-cyclodextrin (HPβCD**)** and *Lippia origanoides* essential oil (EO) as supplied, physical mixtures (PMs) and the inclusion complexes of TML or EO obtained by the different methodologies, together with percentage of mass loss in each peak. FD: Freeze Drying; SD: Spray Drying; RE: Rotary-evaporation; $SCCO_2$: Supercritic CO_2.

In samples processed by the different methods, in turn, changes were observed in the temperature ranges at which these mass losses occurred with a substantial retardation of the TML evaporation to higher temperatures (Figure 4.4).

The temperature ranges of TML evaporation obtained from DrTG, apart from provide information about complexation, also represent a direct measurement of how these complexes could stabilize the TML under heating conditions. This information is of highly importance for this study, since the NLC that will be elaborated undergo heating at 80 °C. Thus, the

stabilization of the TML in the complexed form can be a primordial condition to obtain NLC systems with appropriate drug content.

The first derivative of TG allows to distinguish different stages of mass loss in the samples according to the limits of the peaks obtained. Invariably, all processed samples presented three stages of mass loss between 40 and 280 °C. However variations in both temperature ranges and mass loss associated with each step occurred depending of the method used to produce the inclusion complexes. Specifically, the first loss of mass with T_{peak} close to 60 °C is assigned to the evaporation of the non-complexed TML fraction and the dehydration of HPβCD. The other two steps of mass loss refer to TML evaporation that are interacting with the CD at different levels. The mass loss in the range of 100 to 200 °C may be related to TML-CD associations without drug encapsulation or with partial drug encapsulation, whereas the last step of mass loss that extends the evaporation of TML at temperatures ranges from 200 to 280 °C may be attributed to an real inclusion complexes (KURKOV, LOFTSSON, 2013).

Comparing the methods, SD produced the lowest results of TML evaporation in temperatures above 100 °C, confirming the limited drug encapsulation obtained following this procedure, which is corroborated by the drug content results. The samples processed by $SCCO_2$, in turn, showed intermediate values of evaporation in the temperature ranges of drug-CD interaction, proving the presence of inclusion complexes in a certain amount in these samples.

In contrast, RE produced expressive results of drug-CD interaction in which practically all TML was stabilized either in partial or total encapsulation. However, undoubtedly, FD could produce the largest amount of true inclusion complexes using both EO or TML. In fact, the mass loss in the last evaporation step of FD samples corresponded to almost 70% of the TML available.

Thus, although there were evidences of inclusion complex formation from all methods tested, which was corroborated by the physicochemical results discussed so far, TG data were quite expressive in showing the production methods RE and FD, especially the last one, promoted a superior stabilization of this volatile compound up to a drastic temperature of 280 °C.

Lastly, dissolution assays were performed as additional test to compare the complexation methods used in this work. Indeed, one of the most described effects for CDs inclusion complexes formation refers to changes in the dissolution profile (SÁ-BARRETO et al., 2013).

A significant improvement on the TML dissolution rate occurred for samples produced by any of the methods tested (Figure 4.5). $SCCO_2$ samples presented a slower solubilization than samples obtained by RE, SD and FD, in agreement with thermal analysis result which suggested

a lower complexation using this procedure. In the case of the samples prepared with EO, there was a visual distinction between the dissolution profiles in accordance to TML samples, however without statistical discrimination. An enhancing in the dissolution rate of inclusion complexes with poorly soluble drugs is expected once the encapsulation keeps the hydrophobic guest molecule on the internal environment of the CD and its external hydrophilic portion interacts with the water, increasing, consequently, the dissolution of the complexes (SÁ-BARRETO et al., 2013).

The dissolution results are in line with the other tests performed. Moreover, it is possible to distinguish between the complexation methodologies, and once again, the FD method presented the highest mean values of ED30 for its resulted complex. Thus, this sample was selected to be incorporated into the NLC in the next phase of the study.

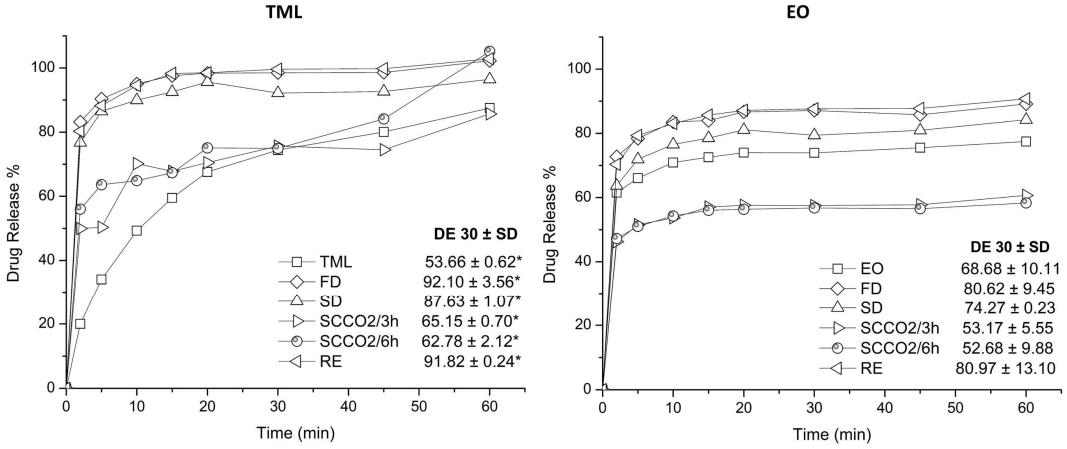

Figure 4.5 Dissolution profile of thymol (TML) and *Lippia origanoides* essential oil (EO) as supplied, physical mixtures (PMs) and the inclusion complexes of TML or EO obtained by the different methodologies, together with dissolution efficiency at 30 min (DE 30). FD: Freeze Drying; SD: Spray Drying; RE: Rotary-evaporation; $SCCO_2$: Supercritic CO_2.

4.4.3. Preparation and analysis of NLC

In order to evaluate the influence of the FD inclusion complexes in the preparation and behavior of the lipid nanoparticles, NLC containing TML or EO in its free form and in complexes were prepared. The particle characterization data are showed in Table 4.3.

Table 4.3 Characterization data. For each NLC: Size of the particle; polydispersity index (PDI); entrapment efficiency (EE); drug loading (DL); and pH.

Sample	*Size (nm ± SD)*	*PDI (± SD)*	*Zeta Potential (mV)*	*EE (% ± SD)*	*DL (% ± SD)*	*pH*
Empty NLC	469.6 ± 26.3	0.410 ± 0.07	-35.8 ± 0.8	-	-	5.6
NLC TML	499.2 ± 28.2	0.473 ± 0.05	-35.8 ± 0.1	97.2 ± 3.1	4.20 ± 3.1	5.6
NLC TML-CD	498.6 ± 31.4	0.426 ± 0.04	-41.9 ± 0.5	95.4 ± 1.8	2.82 ± 1.8	5.6
NLC EO	510.8 ± 16.0	0.469 ± 0.05	-37.5 ± 0.2	98.8 ± 2.9	3.28 ± 2.9	5.6
NLC EO-CD	325.9 ± 5.9	0.518 ± 0.04	-37.7 ± 0.3	76.4 ± 3.1	2.42 ± 3.1	5.6

An unimodal particle sizes distribution was observed with an average particle size in the range from 325 to 510 nm and despite the high values of PDI the measures are within the usual values described for NLC (CIRRI et al., 2012). The zeta potential showed values higher than -35.8 mV, indicating static stability of the produced particles (GHARIB et al., 2015).

The EE, were very high for NLC prepared with free TML or EO due the affinity between the lipophilic TML and the lipids. In contrast, NLC prepared with inclusion complexes showed a reduction in EE, especially with NLC EO-CD, probably due the relative reduction in drug lipophilicity caused by the complexation (CHEN et al., 2014). DL results were within expected range considering the theoretical composition used in NLC preparation. The pH values for NLC was the same of the aqueous vehicle since there is no ionization of TML or HPβCD (Table 3).

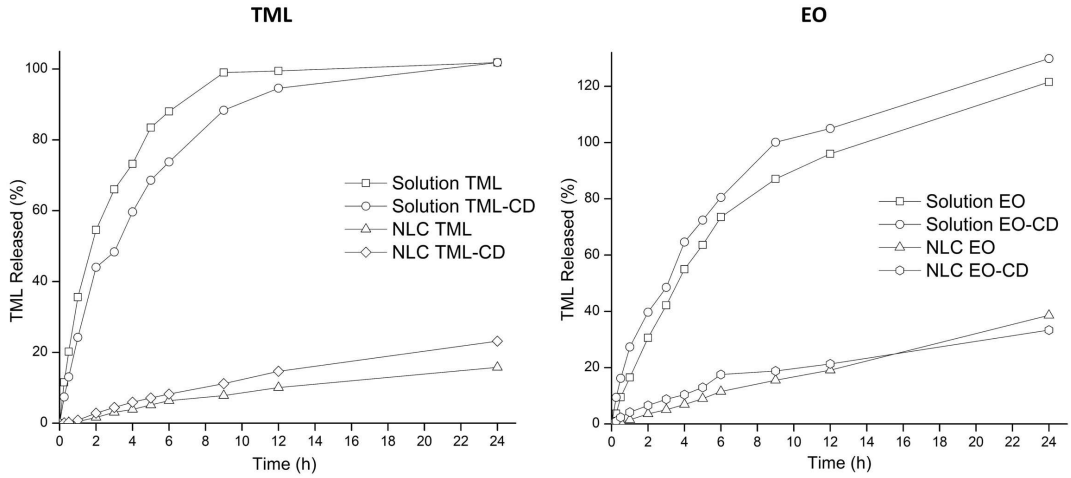

Figure 4.6 Release profile of thymol (TML) and *Lippia origanoides* essential oil (EO) in solution or in nanostructured lipid carriers (NLC), both in non-complexed and complexed form.

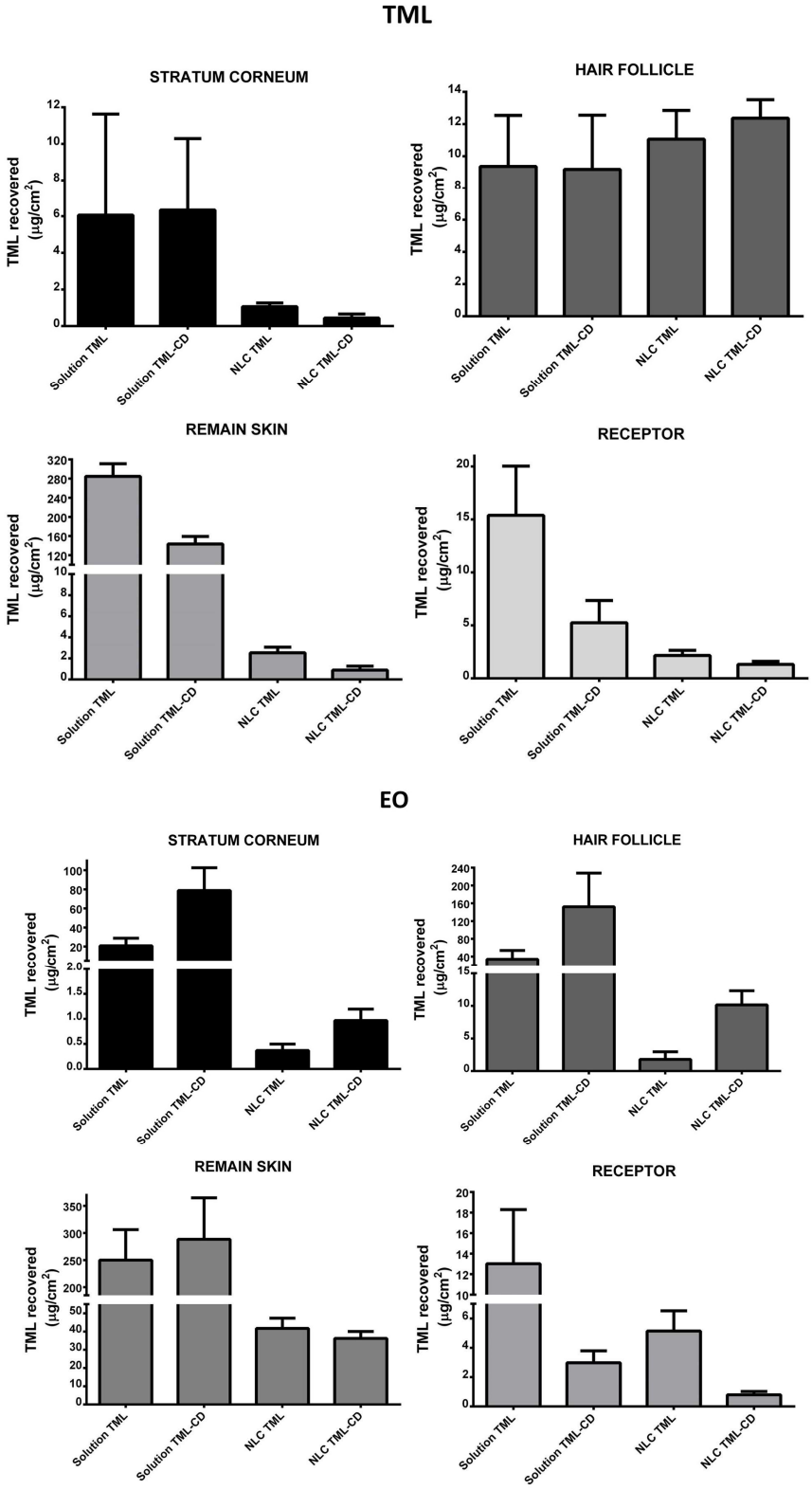

Figure 4.7 Drug recovered from the skin layers and receptor medium after 12h of *in vitro* permeation experiments from thymol (TML) and *Lippia origanoides* essential oil (EO) in solution or in nanostructured lipid carriers (NLC), both in non-complexed and complexed form.

The release profile of free TML and EO, their inclusion complexes, as well as NLC dispersions were exhibited in Figure 4.6. A substantial difference between free TML or EO and their NLC systems was observed. Solutions of TML or EO released all drug content in 12h, whereas NLC showed a controlled drug release with just 20% and 35% of drug content released from NLC produced with TML and EO, respectively at the same period of time. No differences were denoted with the inclusion complexes. The results pointed out the drug control release of NLC due its lipid composition, hindering the drug diffusion even in their complexes in the hydrosoluble form (LIU et al., 2011) and represents a desirable profile with good prospect to a more sustained effect.

According to the permeation results (Figure 4.7), the free TML in solution easily permeated the skin, rapidly accessing the receptor medium, that occours because of the high lipofilisity of TML, resulting in a high affinity with the skin layers and a considerable penetration. The permeation of EO solution in the external skin layers (SC and HF) was higher than with TML solution, which may be explained by the effect of enhancer compounds such as carvacrol (CHEN et al., 2016). Furthermore, the solution of EO containing HPβCD showed an increasing in the amount of drug permeated to the HF and SC, probably due an accumulation of the inclusion complex in this skin appendage and a possible extraction effect of lipids skin caused by CDs, which temporarily decreases this skin barrier (MASSON et al., 1999).

On the other hand, the NLC controled the permeation of the TML and EO, the actives probably have a strong interaction with the lipid components of the NLC making the release more difficult, greatly reducing the drug that penetrate skin and reach receptor medium (Figure 4.7). Specifically, the amount of drug permeated into the RS was reduced by up to 100-fold. In such systems, the lipophilic drug is retained in the nanoparticle lipid matrix and diffuses slowly out of this system (MAESTRELLI et al., 2005).

Interestingly, the reduction in drug permeation in HF was smaller in the case of NLC produced with EO and simple did not occur with NLC prepared with TML isolated. Furthermore, the ratio between the amount of drug permeated in the RS and HF (RS/HF) was drastically reduced from 44.7 of solution TML-CD to 0.07 of NLC TML-CD. Probably, the size of the complex and the reduction in lipophilicity of the complexed drug favors its entry through the follicular route and consequently hindering the permeation through SC (CHEN et al., 2014).

In addition, a synergistic effect between NLC and HPβCD in controling the drug permeation is observed (Figure 4.7). In these lipid matrix, HPβCD decreased the TML penetration in both RS and receptor medium. In the case of NLC TML-CD, the amount of drug

permeated into RS was reduced by more than 315 times. A marked reduction of more than an order of magnitude are also observed in the amount of drug that reaches the receptor medium from the NLC with CD produced with both TML isolated and EO. Indeed, the complexation of the drug included in a lipid matrix represented a further obstacle for its permeation through the skin (GHARIB et al., 2015)

The uncontrolled drug permeation from free TML or EO could, evidently, compromise a topic treatment and even cause toxic effects. TML and essential oils containing TML are capable to generate significant pharmacological effects at low doses (MARCHESE et al., 2016), therefore a prolonged release is a more viable option for topical administration of TML and essential oils. Apart from the benefits of a drug control release achieved by NLC, its functionalized form with CD inclusion complexes could even reduce the drug in receptor medium, reinforcing the advantages of such system for topical proposals.

4.5 CONCLUSION

The CD type and the method of production are decisive factors for a satisfactory formation of inclusion complexes with TML and its natural substrate (EO). Indeed, a better complexation efficiency was achieved using HPβCD, while the freeze-drying method proved to be more effective in produce true inclusion complexes in solid state.

The encapsulation with HPβCD could overcome the volatility and low aqueous solubility of TML and the insertion of these complexes into NLC controled the release and the permeation of TML. Moreover, the inclusion complexes altered the permeation dynamics of TML in the skin, keeping its release circumscribed to the skin initial layers, vectoring the topical treatment. Thus, the NLC systems with inclusion complexes demonstrated to be a viable alternative for the production of stable systems based on TML with potential for a safe and effective topical control release treatment.

3.7 ACKNOWLEDGMENTS

This research was supported by Brazilian agencies CNPq, CAPES and FAP-DF. The authors would like to thank Professor Joyce da Silva from the Laboratory of Natural Products of the Federal University of Pará, Brazil for kindly supplying essential oil extracts used in the work. Additionally, the authors thank Ashland for the cyclodextrins donation.

3.7 REFERENCES

ADEOYE, O.; CABRAL-MARQUES, H. Cyclodextrin nanosystems in oral drug delivery: A mini review. **Int J Pharm.** v. 531, p. 521-531; 2017.

ANGELO, T.; PIRES, F. Q.; GELFUSO, G. M.; DA SILVA, J. K. R.; GRATIERI, T.; CUNHA-FILHO, M. S. S. Development and validation of a selective HPLC-UV method for thymol determination in skin permeation experiments. **Journal of Chromatography B: Analytical Technologies in the Biomedical and Life Sciences**, v. 1022, p. 81–86, 2016.

CHEN, Y.; YANG, X.; ZHAO, L.; ALMSY, L.; GARAMUS, V. M.; WILLUMEIT, R.; ZOU, A. Preparation and characterization of a nanostructured lipid carrier for a poorly soluble drug. **Colloids and Surfaces A: Physicochemical and Engineering Aspects**, v. 455, n. 1, p. 36–43, 2014.

CHEN, J.; JIANG, Q.; CHAI, Y.; ZHANG, H.; PENG, P.; YANG, X. Natural Terpenes as Penetration Enhancers for Transdermal Drug Delivery. **Molecules**, v. 21, p. 1709; 2016.

CIRRI, M.; BRAGAGNI, M.; MENNINI, N.; MURA, P. Development of a new delivery system consisting in "drug - In cyclodextrin - In nanostructured lipid carriers" for ketoprofen topical delivery. **European Journal of Pharmaceutics and Biopharmaceutics**, v. 80, n. 1, p. 46–53, 2012.

CORNAGHI, L.; ARNABOLDI, F.; CALÒ, R.; LANDONI, F.; BARUFFALDI PREIS, W. F.; MARABINI, L.; DONETTI, E. Effects of UV Rays and Thymol/Thymus vulgaris L. Extract in an ex vivo Human Skin Model: Morphological and Genotoxicological Assessment. **Cells Tissues Organs**, v. 201, n. 3, p. 180–192, 2016.

CUNHA-FILHO, M. S. S.; DACUNHA-MARINHO, B.; TORRES-LABANDEIRA, J. J.; MARTINEZ-PACHECO, R.; LANDIN, M. Characterization of β-lapachone and methylated β-cyclodextrin solid-state systems. **AAPS PharmSciTech**, v. 8, n. 3, p. E68-77, 2007.

CUNHA-FILHO, M. S. S.; MARTÍNEZ-PACHECO, R.; LANDIN, M. Effect of storage conditions on the stability of β-lapachone in solid state and in solution. **Journal of Pharmacy and Pharmacology**, v. 65, p. 798–806, 2013.

GELFUSO, G. M.; CUNHA-FILHO, M. S. S.; GRATIERI, T. Nanostructured lipid carriers for targeting drug delivery to the epidermal layer. **Ther. Deliv**, v. 7, n. 11, p. 735–737, 2016.

GHARIB, R.; GREIGE-GERGES, H.; FOURMENTIN, S.; CHARCOSSET, C. AUEZOVA, L. Liposomes incorporating cyclodextrin–drug inclusion complexes: Current state of knowledge. **Carbohydrate Polymers**, v. 129, p. 175-186, 2015.

HIGUCHI, T.; CONNOR, K. A. Phase Solubility Techniques. **Adv. Anal. Chem. Inst.**, v. 4, p. 117–212, 1965.

IQBAL, M. A.; SHADAB, M. D.; SAHNI, J. K.; BABOOTA, S.; DANG, S.; ALI, J. Nanostructured lipid carriers system: Recent advances in drug delivery. **Journal of Drug Targeting**, v. 20, p. 813–830, 2012.

JUNIOR, O. V.; DANTAS, J. H.; BARÃO, C. E.; ZANOELO, E. F.; CARDOZO-FILHO, L.; MORAES, F. F. Formation of inclusion compounds of (+)catechin with β-cyclodextrin in different complexation media: Spectral, thermal and antioxidant properties. **The Journal of Supercritical Fluids**, v. 121, p. 10–18, 2017.

KFOURY, M.; LANDY, D.; RUELLAN, S.; AUEZOVA, L.; GREIGE-GERGES, H.; FOURMENTIN, S. Determination of formation constants and structural characterization of cyclodextrin inclusion complexes with two phenolic isomers: carvacrol and thymol. **Beilstein J Org Chem.** v. 12, p. 29-42. 2016.

KURKOV, S.V.; LOFTSSON T. Cyclodextrins. **Int J Pharm.** 453, p. 167-80. 2013.

LIN, C.; CHEN, F.; YE, T.; ZHANG, L.; ZHANG, W.; LIU, D.; XIONG, W.; YANG, X.; PAN, W. A novel oral delivery system consisting in "drug-in cyclodextrin-in nanostructured lipid carriers" for poorly water-soluble drug: vinpocetine. **Int J Pharm.** v. 465, p. 90-96. 2014.

LIU, D.; LIU, Z.; WANG, L.; ZHANG, C.; ZHANG, N. Nanostructured lipid carriers as novel carrier for parenteral delivery of docetaxel. **Colloids and Surfaces B: Biointerfaces**, v. 85, n. 2, p. 262–269, 2011.

LOFTSSON, T.; HREINSDÓTTIR, D.; MÁSSON, M. Evaluation of cyclodextrin solubilization of drugs. **International Journal of Pharmaceutics**, v. 302, n. 1–2, p. 18–28, 2005.

MAESTRELLI, F.; GONZÁLEZ-RODRÍGUEZ, M. L.; RABASCO, A. M.; MURA, P. Preparation and characterisation of liposomes encapsulating ketoprofen–cyclodextrin complexes for transdermal drug delivery. **International Journal of Pharmaceutics,** v. 298, p. 55-67, 2005.

MÁSSON, M.; LOFTSSON, T.; MÁSSON, G.; STEFÁNSSON, E. Cyclodextrins as permeation enhancers: some theoretical evaluations and in vitro testing. **J. Control. Rel.,** v. 59, p. 107–118, 1999.

MARCHESE, A.; ORHAN, I. E.; DAGLIA, M.; BARBIERI, R.; LORENZO, A. DI; NABAVI, S. F.; GORTZI, O.; IZADI, M.; NABAVI, S. M. Antibacterial and antifungal activities of thymol: a brief review of the literature. **Food Chemistry**, v. 210, p. 402–414, 2016.

MARRETO, R. N.; ALMEIDA, E. E. C. V; ALVES, P. B.; NICULAU, E. S.; NUNES, R. S.; MATOS, C. R. S.; ARAÚJO, A. A. S. Thermal analysis and gas chromatography coupled mass spectrometry analyses of hydroxypropyl-β-cyclodextrin inclusion complex containing Lippia gracilis essential oil. **Thermochimica Acta**, v. 475, n. 1–2, p. 53–58, 2008.

MAXIMIANO, F. P.; COSTA, G. H. Y.; DE SÁ BARRETO, L. C. L.; BAHIA, M. T.; CUNHA-FILHO, M. S. S. Development of effervescent tablets containing benznidazole complexed with cyclodextrin. **Journal of Pharmacy and Pharmacology**, v. 63, n. 6, p. 786–793, 2011.

MENNINI, N.; CIRRI, M.; MAESTRELLI, F.; MURA, P. Comparison of liposomal and NLC (nanostructured lipid carrier) formulations for improving the transdermal delivery of oxaprozin: Effect of cyclodextrin complexation. **International Journal of Pharmaceutics**, v. 515, p. 684-

691, 2016.

MURA, P. Analytical techniques for characterization of cyclodextrin complexes in the solid state: A review. **Journal of Pharmaceutical and Biomedical Analysis**, v. 113, p. 226-238, 2015.

NIEDDU, M.; RASSU, G.; BOATTO, G.; BOSI, P.; TREVISI, P.; GIUNCHEDI, P.; CARTA, A.; GAVINI, E. Improvement of thymol properties by complexation with cyclodextrins: In vitro and in vivo studies. **Carbohydrate Polymers**, v. 102, n. 1, p. 393–399, 2014.

PEREIRA, M. N.; SCHULTE, H. L.; DUARTE, N.; LIMA, E. M.; SÁ-BARRETO, L. L.; GRATIERI, T.; GELFUSO, G. M.; CUNHA-FILHO, M. S. S. Solid effervescent formulations as new approach for topical minoxidil delivery. **European Journal of Pharmaceutical Sciences**, v. 96, p. 411–419, 2017.

PIRES, F. Q.; ANGELO, T.; SILVA, J. K. R.; SÁ-BARRETO, L. C. L.; LIMA, E. M.; GELFUSO, G. M.; GRATIERI, T.; CUNHA-FILHO, M. S. S. Use of mixture design in drug-excipient compatibility determinations: Thymol nanoparticles case study. **Journal of Pharmaceutical and Biomedical Analysis**, v. 137, p. 196–203, 2017.

SÁ-BARRETO, L. C. L.; GUSTMANN, P. C.; GARCIA, F. S.; MAXIMIANO, F. P.; NOVACK, K. M.; CUNHA-FILHO, M. S. S. Modulated dissolution rate from the inclusion complex of antichagasic benznidazole and cyclodextrin using hydrophilic polymer. **Pharmaceutical Development and Technology**, v. 18, n. 5, p. 1035–1041, 2013.

SALÚSTIO, P. J.; FEIO, G.; FIGUEIRINHAS, J. L.; PINTO, J. F.; CABRAL MARQUES, H. M. The influence of the preparation methods on the inclusion of model drugs in a β-cyclodextrin cavity. **European Journal of Pharmaceutics and Biopharmaceutics**, v. 71, n. 2, p. 377–386, 2009.

TAO, F.; HILL, L. E.; PENG, Y.; GOMES, C. L. Synthesis and characterization of β-cyclodextrin inclusion complexes of thymol and thyme oil for antimicrobial delivery applications. **LWT - Food Science and Technology**, v. 59, n. 1, p. 247–255, 2014.

CHAPTER 5 – FINAL CONSIDERATIONS

A HPLC-UV analytical method was developed for TML determination. The method was selective against skin contaminants and presented recovery rates higher than 90% from skin layers. The validation showed the method might be suitable for *in vitro* permeation studies of topical products containing TML.

TML-excipient compatibility studies using a mixture design protocol were useful to provide more complete information on drug stability profile and guide the development of NLC stable formulations, preventing the use of incompatible components such as TAU, which presented a synergic effect with the other components of NLC, reducing the TML stability.

The process of complexation with CDs was able to manipulate successfully the physicochemical characteristics of TML and EO, originating a more stable product, therefore enhancing the amplitude of its applications.

The CD type and the method of production are decisive factors for a satisfactory formation of inclusion complexes with TML and its natural substrate (EO). Indeed, a better complexation efficiency was achieved using HPβCD, while the freeze-drying method proved to be more effective in produce true inclusion complexes in solid state.

The encapsulation with HPβCD was able to overcome the volatility and low aqueous solubility of TML and the insertion of these complexes into NLC was able to control the release and the permeation of the active component. Moreover, the inclusion complexes altered the permeation dynamics of TML in the skin, keeping its release circumscribed to the skin initial layers, vectoring the topical treatment.

Thus, the NLC systems functionalized with inclusion complexes demonstrated to be a viable alternative for the production of stable systems based on TML with potential for a safe and effective topical control release treatment.